PREPARATION AND CHARACTERIZATION OF ULTRA-THIN FILMS CONTAINING Au AND Ag NANOPARTICLES USING LAYER-BY-LAYER DEPOSITION TECHNIQUE

A THESIS

SUBMITTED TO THE DEPARTMENT OF CHEMISTRY

AND THE INSTITUTE OF ENGINEERING AND SCIENCES

OF BİLKENT UNIVERSITY

IN PARTIAL FULFILLMENT OF THE REQUIREMENTS

FOR THE DEGREE OF

MASTER OF SCIENCE

By

CAN PINAR CÖNGER

July 2009

I certify that I have read this thesis and that in my opinion is it is fully adequate, in scope and quality, as a thesis of the degree of Master in Science

.....

Prof. Dr. Şefik Süzer (Principal Advisor)

I certify that I have read this thesis and that in my opinion is it is fully adequate, in scope and quality, as a thesis of the degree of Master in Science

.....

Prof. Dr. Duygu Kısakürek

I certify that I have read this thesis and that in my opinion is it is fully adequate, in scope and quality, as a thesis of the degree of Master in Science

.....

Assist. Prof. Dr. Oğuz Gülseren

I certify that I have read this thesis and that in my opinion is it is fully adequate, in scope and quality, as a thesis of the degree of Master in Science

.....

Assist. Prof. Dr. Dönüş Tuncel

I certify that I have read this thesis and that in my opinion is it is fully adequate, in scope and quality, as a thesis of the degree of Master in Science

.....

Dr. Gülay Ertaş

Approved for the Institute of Engineering and Science

……..

Prof. Dr. Mehmet Baray

Dirtector of Institute of Engineering and Science

ABSTRACT

PREPARATION AND CHARACTERIZATION OF ULTRA-THIN FILMS CONTAINING Au AND Ag NANOPARTICLES USING LAYER-BY-LAYER DEPOSITION TECHNIQUE

CAN PINAR CÖNGER

M.S. in Chemistry

Supervisor: Prof. Dr. Şefik Süzer

July, 2009

The main objective of this thesis is to investigate the layer-by-layer deposited polyelectrolyte and polyelectrolyte/metal nanoparticle films by using X-ray Photoelectron (XPS) and Optical Spectroscopy (UV-Vis).

Within this purpose, in the first part of the study, layer-by-layer deposited single and oppositely charged bilayered films are investigated by XPS. To extract additional information in the molecular level, the samples are analyzed while applying an external voltage bias. It is shown that applying external electrical stimuli to a single polyelectrolyte layer coated Si/SiO_2 system responds to the change in the polarity by molecular rearrangements, evidenced by the changes only in the intensity of the corresponding $–N^+(1s)$ peak.

In the second part of the study, metal nanoparticle (Au and/or Ag) incorporated polyelectrolyte films are investigated by optical spectroscopy. Within this frame, multilayer gold and silver nanaoparticle/polyelectrolyte films are prepared both separately and in bimetallic form. In order to get further understanding about the optical responses of single type of metal nanoparticle incorporated systems, several experimental approaches are followed. These approaches also enable us to control and manipulate the optical properties of these compact structures.

The last part focuses on incorporation of metallic ions into layer-by-layer assembled polyelectrolyte matrices through ion-exchange method. It is shown that metal ions can be incorporated and subsequently reduced within this polymer matrix by UV or X-ray irradiation and can also form nanoparticles.

Keywords: Layer-by-Layer Deposition, Polyelectrolytes, Au and Ag Nanoparticles, Surface Plasmon Resonance, Interlayer Interparticle Interaction, Ion-Exchange, XPS.

ÖZET

KATMAN-KATMAN KAPLAMA YÖNTEMİYLE Au VE Ag NANOPARÇACIKLARI İÇEREN ULTRA-İNCE FİLMLERİN HAZIRLANMASI VE KARAKTERİZASYONU

CAN PINAR CÖNGER

Kimya Yüksek Lisans Tezi

Danışman: Prof. Dr. Şefik Süzer

Temmuz 2009

Bu tezin ana amacı katman-katman kaplama yöntemiyle kaplanan polielektrolit ve polielektrolit/metal nanoparçacık çiftlerinin X-ışını Fotoelektron (XPS) ve Optik Spektroskopi (UV-Vis) yöntemleriyle incelenmesidir.

Bu amaç kapsamında, çalışmanın ilk kısmında katman-katman kaplama yöntemiyle kaplanan tek ve zıt yüklü iki polielektrolit katmanlı filimler XPS yöntemiyle incelenmiştir. Ayrıca, moleküler düzeyde daha fazla bilgi edinebilmek amacıyla, örneklere dışarıdan voltaj uygulanmıştır. Si/SiO_2 alttaşı üzerine kaplanan tek bir polielektrolit katmanı dışarıdan elektriksel olarak uyarılmış ve bu sistemin değişken polariteye bağlı olarak moleküler olarak yeniden düzenlendiği, ilgili - $N^+(1s)$ tepeciklerindeki intensite değişimleriyle kanıtlanmıştır.

Çalışmanın ikinci kısmında, metal nanoparçacık (Au ve/veya Ag) dahil edilmiş polielektrolit filmleri optik spektroskopik yöntemle incelenmiştir. Bu

çerçevede, çok katmanlı altın ve gümüş nanoparçacık/polielektrolit filmleri ayrı ayrı ve bimetalik formlarda hazırlanmıştır. Tek tip nanoparçacık dahil edilmiş polielektrolit filmlerinin optik özellikleri hakkında daha fazla bilgi edinebilmek amacıyla, birkaç deneysel yaklaşım takip edilmiştir. Bu yaklaşımlar bize aynı zamanda bu çok katmanlı yapıların optik özelliklerini kontrol etme ve yönlendirme olanağını sağlamıştır.

Çalışmanın son kısmı iyon değişimi yöntemiyle metal iyonları dâhil edilmiş katman-katman kaplama metoduyla hazırlanmış polielektrolit matrislerine odaklanmıştır. Metal iyonlarının sisteme ne derece dahil edilebildiği, UV ve/veya X-ışınlarına maruz bırakılarak polimer matrisi içerisinde indirgenmesi ve nanoparçacık oluşumu ile incelenmiştir.

Anahtar Kelimeler: Katman-Katman Kaplama, Polielektrolitler, Au ve Ag Nanoparçacıkları, Yüzey Plasmon Rezonans, Katmanlar Arası Etkileşim, XPS.

LIST OF ABBREVATIONS

LbL: Layer-by-Layer

LB: Langmuir-Blodgett

NP: Nanoparticle

PAH: Poly(allyamine hydrochloride)

PEI: Poly(ethylenimine)

PMMA: Poly(methyl methacrylate)

PSS: Poly(sodium 4-styrene-sulfonate)

QCM: Quartz Crystal Microbalance

SAM: Self Assembled Monolayer

SEM: Scanning Electron Microscope

SPR: Surface Plasmon Resonance

UV-Vis: Ultraviolet-Visible

WCA: Water Contact Angle

XPS: X-ray Photoelectron Spectroscopy

ACKNOWLEDGEMENTS

At the end of this comprehensive scientific study and education, I want to express my deepest thanks to Prof. Şefik Süzer for his supervision and guidance throughout these studies for the last three years.

I would thank to our past and current lab group members Hikmet Sezen, Dr. Ivalina Abramova, Eda Özkaraoğlu and special thanks to Hacı Osman Güvenç and İlknur Tunç.

I would also like to thank to Chemistry Department members Emine Yiğit and Ethem Anber.

I will always remember my dear friends Esra Gülser, S. Altuğ Poyraz, Mustafa Sayın, Abidin Balan, Alper Kılıklı, Halil İbrahim Okur, Fahri Alkan.

My family has a special meaning in my life. I am grateful to my mother who watches over me like an angel, my father for his endless moral support, my sister and my brother in law for their unconditional love and sacrifice.

Finally, I want to dedicate this thesis to my dearest grandfather Yaşar Özkan.

TABLE OF CONTENTS

LIST OF FIGURES

1. INTRODUCTION

Surface coating has always been a very important synthetic route for introducing new functionalities to the materials' surfaces, while conserving the bulk features of the underlying support. Developing new strategies for surface coating opened an interdisciplinary field for scientists and engineers that embrace polymeric, organic, inorganic and biological components. From the technological aspect, it is always desirable to introduce multi-functionalities to the surfaces. Polymeric materials attracted particular attention for the surface modification because of the known versatility of polymers. A very recent approach fulfills the expectations of preparing functional surfaces where arrangements of organic molecules can be controlled in nanoscopic level. The method introduces deposition of single molecular layers in a consecutive manner to form multicomposite structures, the so-called "Layer-by-Layer (LbL) Deposition".

1.1 Layer-by-Layer Deposition

For about 60 years, new approaches aim to tailor the materials' surfaces are dominated by the Langmuir-Blodgett (LB) technique. In this method, monolayers are first formed on a water interface and then transferred onto a solid support subsequently.[1] In the late 1960s, by using LB technique, Kuhn and co-workers pioneered fabrication of synthetic heterostructures of organic molecules.[2] They demonstrated that monomolecular layer systems can form functional units which exhibit different properties than individual layers. They also showed for the first time

that individual layers can be manipulated in nanoscale by using donor and acceptor dyes in different layers of the LB films.

However, scientists were seeking for an alternative method for thin-film formation since LB technique suffered from the limitations with respect to substrate size, topology and film stability. In 1966, a promising work was proposed by Iler where multilayer structures can be constructed by using charged inorganic colloids.[1] Although the work did not attract much attention of scientists at that time, it created the basic principles of multilayer formation processes for next generation experiments.

In the early 1990s, Decher's group introduced a technique for the fabrication of the multicomposite films which is based on the electrostatic attraction between the oppositely charges species.[1,3,4] The method has encountered a strongly increasing interest for establishing nanoarchitecture films due to the ease of the process and the independency on nature, size and topology of the substrate. Moreover, the technique has proven its usefulness, in a wide variety of charge supporting building block materials like macromolecules,[2] biomacromolecules such as proteins and DNA,[5] colloidal particles, etc. Complex functionality of layer-by-layer assembled films give application access by tailoring the surface interactions and choosing materials used such as light-emitting thin films, permselective gas membranes, electrochromic films, electrocatalysis, sensors, anti-corrosive coatings, etc.[2] The basic building blocks of the LbL technique are the charged polyelectrolytes.

1.1.1 Polyelectrolytes

Polyelectrolytes have found numerous applications in the fields of science and engineering as well as their functions in cellular mechanisms in the form of proteins, polypeptides and nucleic acids. Applications in the field of chemistry mainly focused on polymer interface, materials, analytical and colloidal chemistry. A polyelectrolyte is defined as a macromolecular species that dissociates into a charged polymeric molecule when it is placed into an ionizing solvent. In order to conserve the electroneutrality, dissociation is accompanied by smaller oppositely charged counterions to neutralize the charge on the repeating unit.[6-8] Ionic strength of the solution is an important factor for tuning the form of the polyelectrolyte. As it is depicted in Figure 1, if the ionic strength of the solution is low, this macromolecular specie tends to be in its most expanded form owing to the intramolecular repulsion on each monomeric unit.[9] Conversely, in the high ionic strength solutions, a polyelectrolyte becomes more coiled due to the screening effects of polymer charges by the excess number of counterions in the solution. The significance of this physical property of a polyelectrolyte has been, and will continue to be a major study for experimental and theoretical scientists. The degree of charge screening can be tuned in order to control the thickness, uniformity, stability and permeability of polyelectrolytes and their corresponding layer-by-layer assembled composite structures.

Complexation ability of oppositely polyelectrolytes is an important aspect in terms of the similarities between polyelectrolyte complexes and their corresponding multilayer structures. Schlenoff and co-workers showed that polyelectrolytes and

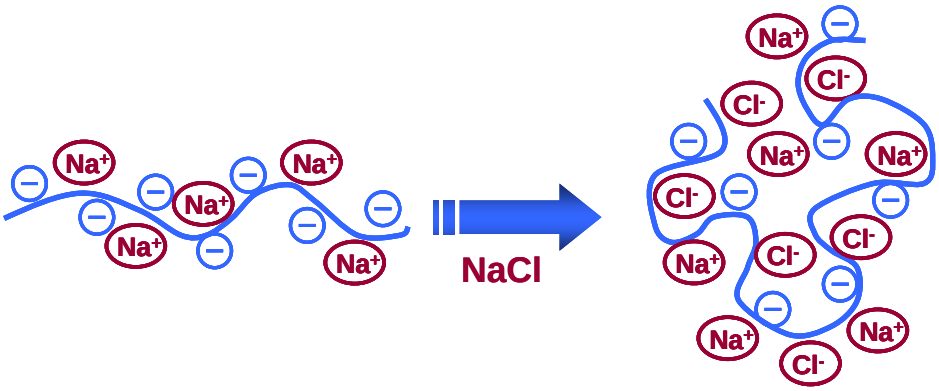

Figure 1. Illustration of the effect of the ionic strength on polyelectrolyte shape.[10]

their multilayer structures contribute to similar characteristics like internal structure, physical structure and morphology.[11] Charges on the monomeric units can be balanced by either "intrinsic compensation" or "extrinsic compensation". The term intrinsic compensation refers to balancing the charge units of polymer chain with an oppositely charged polyelectrolyte. However, in the presence of an external salt solution, salt counterions tend to equilibrate the net charge by entering the bulk of the complex and convert it to extrinsically compensated state.[12] Polyelectrolyte multilayers share the same properties where they form structured and compatible depositions on different substrates. It has been also shown that polyelectrolyte solutions and their multilayer structures can not even be distinguished by X-ray diffraction method because of the highly interpenetration properties of multilayer complexes in molecular level because of the absence of Bragg peaks.[12]

Due to the ability to reach any pores or cracks on supporting surface without blocking their openings[2], polyelectrolytes are superior on ready made solids or colloidal complexes on assembly processes. Beside these accessibility characteristics, polyelectrolytes have found numerous application areas like

ultrafiltration membranes, fuel cell membranes, environmental detectors and chemical sensors, etc.[2]

1.1.2 Polyelectrolyte Adsorption and Multilayer Formation

Interfacial properties of the materials are still great challenge for scientists. Polymer adsorption provides prevailing tools for investigating the interfacial properties. Although the thickness of a polymer layer depends on the nature of the substrate and polymer, it is always restricted by the amount of adsorbed polymer.[13] If adsorption process is applied in a dilute solution, the size of a polymer layer does not surpass the polymer size in the bulk solution. This limitation brings about that thick films can not be constructed by using simple adsorption in molecular level. By using layer-by-layer deposited multilayer concept, one can obtain relatively thick films with a rather well-controlled thickness in molecular level. This perception introduces most versatile and efficient ways for the formation of films with a well-controlled thickness and necessary characteristics.

Inversion and successive renovation of the surface properties is a key for a successful deposition of multilayer films. The method is very simple and versatile as demonstrated in Figure 2 for subsequent deposition of polycation (positively charged)-polyanion (negatively charged) couples on a negatively charged substrate. The process is driven by strong electrostatic forces between charged substrate and oppositely charged species that is prepared from its solution. Single monomolecular layers can be constructed alternately on any charged objects independently from its nature, size and topology. A schematic representation of multilayer formation depicts the adsorption of a polycation and polyanion on a negatively charged substrate, respectively. Two common polyelectrolytes are used in the illustration as building

blocks; Poly(allylamine hydrochloride) as a polycation and poly(styrene sulfonate) as a polyanion (Figure 2C). Because polyelectrolytes can reach any pores or cracks on substrate and coat them without clogging their openings, surface charge is overcompensated by the adsorbed polymer layer in each deposited layer. ζ potential measurements also verifies this charge overcompensation,[14] thus one can adsorb another polymer layer that is oppositely charged. Concentrations of the polyelectrolyte solutions are typically in the ranges of several milligrams per milliliters. The used amounts in multilayer fabrications are much larger than the required. This strategy is followed in order to ensure that solutions do not become exhausted during the construction of films involving hundreds of layers.

After adsorption of each layer, washing procedure is used in order to remove the weakly bounded molecules which also stabilize the adsorbed polymer layers.[15] This process also ensures no free polyelectrolytes interact in solution with other components. Different deposition times are reported in the literature from minutes to hours. In the case of polyelectrolyte adsorption, several minutes are sufficient to terminate the deposition step[15,16] where for metallic cluster e.g. gold colloids, hours are needed depending also on their concentrations.[17,18]

In the LbL processing, most commonly used substrates for the deposition are flat surfaces. In order to coat large surfaces, new methods were utilized. For this purpose, Schlenoff introduced the spraying method where solutions of oppositely charged polyelectrolytes are sprayed onto a vertically held sample in an alternative fashion.[19] Similarly, spin coating method was introduced to LbL deposition that was demonstrated by Hong[20,21] and by Weng.[22] In both approaches, the amount of polyelectrolyte solution to coat the large surfaces is much less then the classical

layer-by-layer deposition. Thus, both of these new methods are expected to contribute to the general acceptance of the technology.

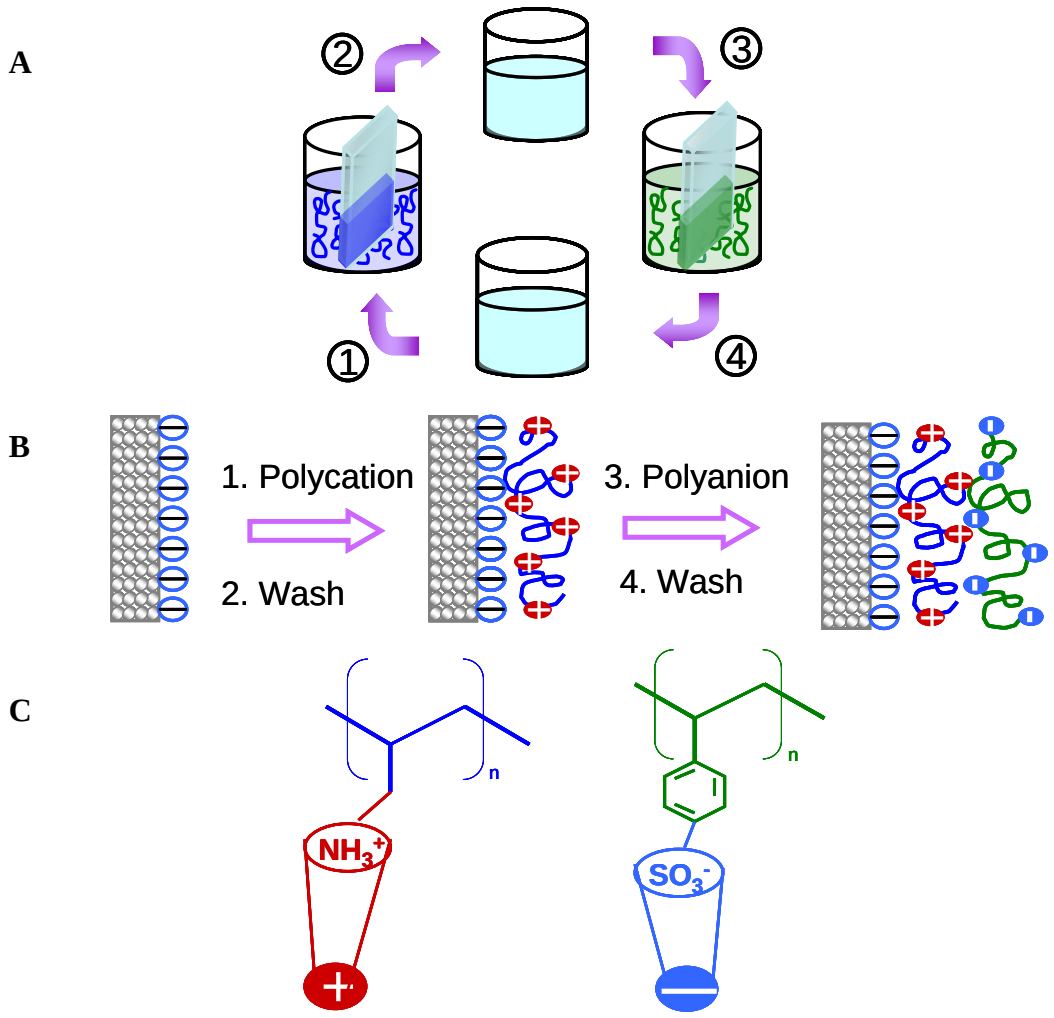

Figure 2. **(A)** Schematic representation of polyelectrolyte adsorption on a substrate. Steps 1-3 depict the polycation and polyanion adsorption respectively. Steps 2-4 show washing processes. **(B)** Molecular illustration for polyelectrolyte deposition on a negatively charged substrate. **(C)** Molecular structures for the most commonly used polyelectrolytes: Poly(allylamine hydrochloride) and Poly(stryrene sulfonate) sodium salt.

1.1.3 Ion-Exchange Chemistry in Multilayers

Incorporation of metal ions into various matrices and surfaces using mostly easy and economical chemical processes is a key synthetic route for numerous applications like catalysis, sensing, biochemical applications etc. The Layer-by-Layer Technique fulfills these expectations since almost any ionic species including synthetic polyelectrolytes, biopolymers, nanoparticles, etc. can be incorporated into multilayer assemblies through the alternating deposition of the oppositely charged species.[1,3,4,23,24]

In most studies including LbL method, it is always desirable to control the surface functionalities of the materials, such as wettability. In a recent study Huck and co-workers showed that wetting characteristics of cationic polyelectrolyte deposited substrates can be modified by choosing a different nature of counterion.[25] Choi et al. demonstrated the formation of Self-Assembled Monolayers (SAMs) presenting imidazolium ions at the tail ends on Au substrate having different anions and the effect of counterions on the surface wettability.[26] It has also been shown that imidazolium ion-terminated monolayers can be assembled on silicon surfaces where water contact angle was increased via exchanging Cl^- counterions with PF_6^- but a complete exchange between counterions takes several hours. The studies were conduced by Niu and co-workers to a further level by achieving a fast exchange between counterions.[27] They applied a small positive potential to polyelectrolyte-functionalized ionic liquid modified ITO. A resulting current was caused by the exchange of the counterions between the interface and the solution. It was shown that the contact angle of the film can be tuned after applying an electric field to the film. In a very recent study Su et al. presented a well-established ion-exchange chemistry

to multilayers assembled by LbL technique using common polyelectrolytes on silicon substrate in order to tune surface wettability.[28] This approach is expected to be applicable to any substrate conferred by the LbL assembly because it involves no chemical modification of the substrate or the polyelectrolytes used.

Recent attempts for incorporating metallic or inorganic ions into multilayer assemblies showed that ionic groups can be created in the multilayer which can bind desired inorgic salt by controlling the pH of the solution during fabrication of the thin films from weak polyelectrolytes.[29] After incorporation of the inorganic salts, they converted to nanoparticles subsequently. As it was shown by our group in a recent study, irradiation by X-ray and 254 nm deep-UV of gold salt in a PMMA film leads to reduction of gold ions and nanocluster formation which is evidenced by both X-Ray Photoelectron Spectroscopy (XPS) and UV-vis-NIR absorption spectroscopy.[30]

1.2 Layer-by-Layer Assembly of Nanoparticles

Metal nanoparticles have attracted a lot of attention because of exhibiting unusual physical and chemical properties that strongly differs from the properties of bulk metals.[31] Thus, these nanoparticles have interesting perspectives in the applications such as biomaterials, biomedicines, catalysts and sensors.[32]

Incorporation of nanoparticles into thin film structures with a well-defined control over chemical and physical properties poses a major confront. In order to produce thin films of metal nanoparticles that can lead to novel application in wide range of applications, numerous methods have been developed. Deposition of nanoparticle layers through Langmuir-Blodgett technique, deposition of nanoparticles via sol-gel chemistry and formation of nanoparticles based on

templating polymeric thin films are some examples for the developed techniques over the years.[33] Despite the establishment of thin films including nanoparticles, assembly of these particles onto a surface having different characteristics e.g. geometry, type has remained as an unsolved problem.

After the development of layer-by-layer deposition method, the technique is utilized and expanded to the preparation of conformal thin films including nanoparticle partnered polyelectrolytes.[20,34-38] The extension of LbL method to incorporation of metal nanoparticles with precise control over film properties, introduced multifunctionality to these nanostructured films by the means of catalytic, magnetic and optical properties.

1.2.1 Optical Properties of Metal Nanoparticles

The fascinating optical properties are one of the most interesting aspects of metallic nanoparticles which strongly depend on particle size and shape. Gold in bulk form exhibits yellow color in reflected light where thin gold films look bluish in transmission. As the particle size of gold decreases, the color changes from several tones of purple and red.[31] The drastic change in color originates from the so-called surface plasmon resonance phenomena.

1.2.1.1 Surface Plasmon Resonance

When the conduction electrons of nanoparticles interact with the incident electromagnetic radiation, they exhibit collective oscillation that dominates the optical properties. For the particles where their sizes are much smaller than wavelengths of the incident light, electrons move in phase in the particle. Based on this knowledge, it is considered that they create a dipole under the influence of the

incident radiation. On each side of the particle, surface polarization charges are generated as a result of the electron motion (Figure 3a). In order to compensate this polarization, a restoring force forms in the nanoparticle which leads to a resonance frequency in the absorption spectrum. The sharp band resulted from this phenomena is termed as surface plasmon resonance. In order to exhibit drastic color effects, the plasma frequency of the nanoparticle has to lie in the visible part of the absorption spectrum. For the metals such as Pb, Cd and Hg, the electrons possess plasmon resonances in the UV part. Additionally, oxidative properties of these metals make the surface plasmon experiments harder. For the case of the metals like Au, Ag and Cu, the plasmon frequency lies in the visible part of the absorption spectrum, therefore surface plasmon experiments are mostly carried out with these metals.

There are additional contributors that affect the resonance frequency, and most of the discussions are focused on the size , shape and nature of the surrounding medium. For the case of the nonspherical particles, for instance rods, the oscillation modes can be either along (longitudinal) or across (transversal) the rod (Figure 3b). Because there is a strong dependence of the resonance wavelength on orientation of the electric field relative to the particle, optical properties are strongly affected.[31]

1.2.1.1.1 Size Dependency

Size dependency of the plasmon frequency of metallic nanoparticles, especially gold nanoparticles, has been widely investigated by various groups.[39-42] Particles having diameters smaller than 5 nm do not exhibit appreciable plasmon absorption.[43] As size of the particle becomes larger than 5 nm, the absorption band covers the visible region.[43] It is known that 5-50 nm silver and gold nanoparticles have strong absorption bands at around 390-420 nm and 520-560 nm, respectively.[44]

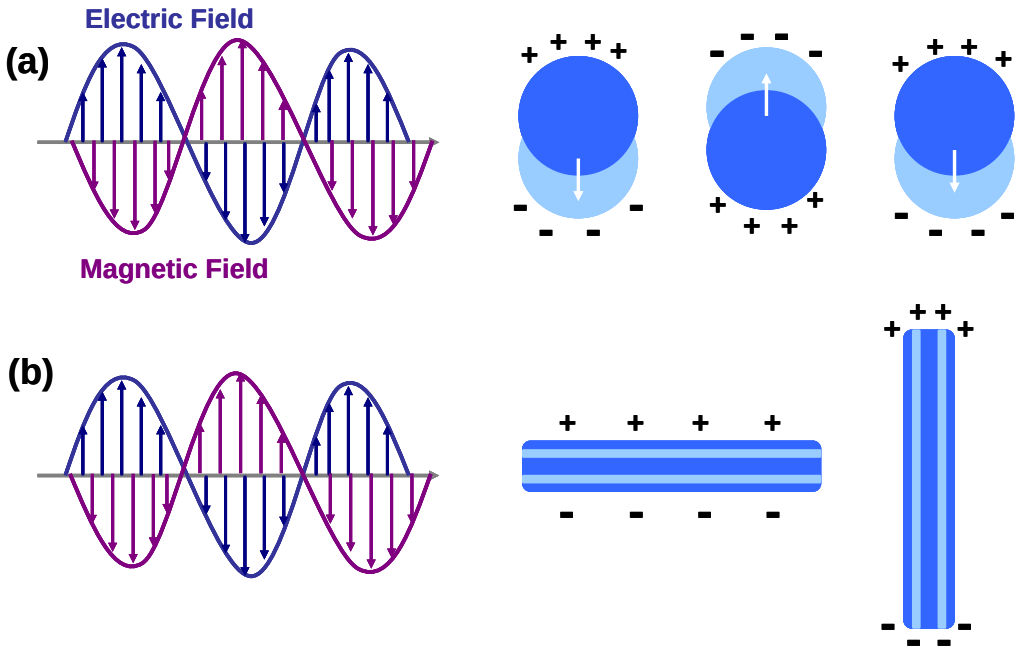

Figure 3. (a) Schematic representation for the metal nanoparticles that are interacting with the electromagnetic radiation. **(b)** Oscillation modes for a metal nanorod: Transverse and longitudinal oscillations respectively.

When the size of the nanoparticles increase, i.e. >25 nm, the plasmon bands start to broaden and red-shifted.[44] The change in the position and the shape of the absorption band is explained by El-Sayed[44] as inhomogeneous polarization of particles by the electromagnetic field. It is said that, as the particle size increases, dimensions of the nanoparticles becomes comparable with the wavelength of the interacting light.

1.2.1.1.2 Composition Dependency

Combination of the metal nanoparticles in different combination has gained an increasing attention in recent years. For tailoring surface plasmons, bimetallic nanoparticles are very important which can be classified into two types. First one is the alloys which stand for the particles of two metals distributed homogeneously.

The other type of the bimetallic nanoparticles is the so-called core-shell nanoparticles. In the case of the core-shell particles, particles of the two metals arrange heterogeneously.

Among the numerous bimetallic systems investigated,[39,42] combination of Au and Ag metals has interesting consequences. Both Au and Ag have sharp absorption bands in the visible part of the spectrum and because they have similar lattice constants in forming fcc crystals, they can form alloy particles in any composition.[45] Alloy nanoparticles are most of the time prepared by simultaneous reduction of the metal salts. A number of groups have studied the relationship between the composition of the Au-Ag alloys and the plasmon absorption band.[44,46,47] They demonstrated that there is a linear dependency between the composition and wavelength of the SPR band. It is shown that the position of the SPR band lies between the absorption band of pure gold and pure silver. Color also changes via changing the composition. As Au content of the alloy increases, the color changes through yellow to red.

Synthesizing core-shell nanoparticles containing gold and silver from different synthetic routes is also presented by various authors.[48,49] These different approaches follow either incorporation using sequential of the metals or segregation during co-reduction. In the case of the core-shell nanoparticles plasmon absorption is mostly determined by the shell. When silver is deposited onto gold, the position of the plasmon band changes drastically, i.e. from 520 nm to 400 nm depending on the shell thickness.[50] This radical change is explained as alteration in the oscillation mode of the surface conduction electrons.

1.2.1.1.3 Surrounding Medium Dependency

The other factor affecting the plasmon absorption of the metal nanoclusters is the surrounding medium. Solvent medium that the nanoparticles are prepared can outcome with two categories: The first group includes the solvents that can modify the refractive index of surrounding nanoparticle and the second group of solvents can complex with the surface of the clusters.[43] In order to understand the solvent phenomena, gold nanopartices are the most investigated.[43,51]

The solvents having no active functional groups, do not interact with the surface of the gold. It is demonstrated that when gold nanoparticles are prepared in such solvents, the absorption band shifts to higher wavelengths with an increase in the refractive index.[43]

When the gold nanoparticles are prepared in polar solvents, the position of the absorption maximum does not change because of the complexing ability of these solvents with gold surfaces. Because gold particles have high electron affinity, they are capable of withdrawing electrons from the solvent.[43] This property leads to stabilize these charged particles by the solvent molecules and prevents aggregation of the particles.

1.2.2 Optical Responses of Metal Nanoparticle Incorporated LbL Films

Controlled tunability of the surface plasmon frequencies of the metal nanoparticles is a key process for the potential applications of the chemical and biosensor technology, advanced spectroscopy and microelectroelectronic devices.[52] The most important parameters that affect the plasmon frequency are the shape of the nanoparticles, surrounding medium and the interparticle distances.[53] Layer-by-layer deposition technique is now the most widely used assembly process for the

incorporation of the metal nanoparticles because of the great flexibility on choosing the substrate, material and controlling the average thickness of the corresponding layers. The first attempt for the preparation of gold nanoparticle-polyelectrolyte films by tunable optical properties was by Calvert and his co-workers.[18] In these films gold nanoparticles were introduced in an organic media which have different dielectric properties. Hence the nanoparticles were subjected to an interaction between this matrix and also with each other, within and between individual layers.[52] The interparticle separation and the dielectric constant of the matrix were thought as the major factors affecting the dipolar-dipolar interactions and resulting surface plasmon resonance. It is usually expected to observe a red-shift in the SPR band of an inorganic nanoparticle when it is intercalated into an organic matrix. In the previous works,[42,54] only one broad absorption peak was observed without separate contributions of individual and collective resonances.

Another effort for incorporating gold nanoparticles into LbL films was presented by Zhang et al.[55] They proposed a new method for fabrication of the gold nanoparticle/polyelectrolyte films. In order to achieve high stability, they utilized the layer-by-layer technique in the assembly step and by a post-photoreaction, the ionic interactions were converted to covalent linkages.[55] By using this method, they claimed that a patterned multilayer surface is achieved containing both organic and inorganic hybrids.

Considering the preparation of the films, interparticle distances between the nanoparticles and the environment that the nanoparticles are embedded, become the most important factors that significantly affect the optical properties of these films. Considering the dilute assemblies of the nanoparticles, it is thought that the refractive index of the surrounding medium is the most important factor.[42] It is recently shown

that for closely packed nanoparticle films on either flat surfaces[56] or on spheres[57], dipole-dipole interactions play a significant role on the optical properties of the nanoparticles. In these closely-packed systems, the determining mechanism for the surface plasmon frequency is the interparticle separation.

In a recent study, Tsukruk et al. demonstrated that organized multilayer films from gold and polyelectrolyte layers can be constructed where individual and collective resonances of gold nanoparticles can be observed separately.[52] They claimed that all films showed a strong extinction peak in the range of 510-550 nm owing to the plasmon absorption of individual gold nanoparticles. However, they observed a contribution of a second strong peak at around 620 and 660 nm for the films including sufficient gold nanoparticle density. They attributed this contribution as the collective plasmon resonance of gold nanoparticles from intralayer coupling (interaction within the layer). Additionally, it is said that under certain conditions interlayer interparticle resonance (interaction between the layers) could be observed distinctly at around 800 nm in the UV-Vis spectra. Similar work was performed by Liz-Marzan and his co-workers where spherical and triangular/hexagonal synthesized gold nanoparticles were embedded into an organic matrix via the layer-by-layer assembly.[58] It was observed that as the number of the gold nanocolloid bilayers increased, a new band developed at 650 nm. This finding was associated with the interaction of the nanoparticles in the adjacent layers.

In order to control the interparticle separation, Liz-Marzan and Mulvaney presented a work using Au(core)@Si(shell) particles in multilayer assemblies.[56,58] Silica was used as a shell material because of its inertness. By varying the shell thickness, they determined the interparticle separation. They observed that as the thickness of the shell increases, the separation between gold nanoparticles increases

which leads to a blue-shift in the plasmon resonance band toward the characteristic of isolated gold nanoparticles.

Preparation of metal nanoparticle/polyelectrolyte multilayers is not limited with substrates and film structures. In the layer-by-layer deposited systems, gold nanoparticles can also be used as templates. Caruso et al. demonstrated that oppositely charged polyelectrolytes can be coated on carboxylic acid derivatized gold nanoparticles.[59] It is shown that, after deposition of each polyelectrolyte layer on gold particles, a systematic red-shift on the SPR was observed. This shift was attributed to the successful coating of polyelectrolyte layers. They have also been shown that the polyelectrolyte functionalized gold nanoparticles can be further deposited onto planar surfaces. So by using this strategy, both solution based multilayers and film structures can be obtained.[59] By using the same approach, Caruso's group also introduced multilayer hollow polyelectrolyte spheres.[60] Alternating deposition of oppositely charged polyelectrolytes on gold nanoparticles yielded stable organic shells after several polymer layers. These metallic cores were then dissolved with cyanide ions. It was claimed that obtained hollow polyelectrolyte multilayer capsules would have very important aspects in functionalized surfaces.

Demonstrations of the metal nanoparticle incorporated layer-by-layer systems showed that, molecular control over the films can tune the optical properties of the nanoparticles. These findings are thought to be very promising for the further scientific and commercial applications.

1.3 X-ray Photoelectron Spectroscopy

X-ray Photoelectron Spectroscopy, XPS, is a powerful technique and one of the most widely used for the surface analysis of the materials. XPS, which is also

known as the ESCA (Electron Spectroscopy for Chemical Analysis) was first discovered by Siegbahn. As a result of the continuous development of various experimental parameter, XPS has become the most popular surface analysis method because of its great ability to give chemical information and sensitivity for solids, thin films and nanostructures.[61]

1.3.1 Principles

XPS is based on the kinetic energy determination of the emitted photoelectrons when the sample under investigation is subjected to highly energetic X-rays as shown schematically in Figure 4. Binding energy of the emitted electro ns is determined by the Einstein's equation:

$$BE = h\upsilon - KE - \Phi \quad (1)$$

where BE corresponds to the binding energy, hυ to energy of the X-ray and KE to kinetic energy of the photoelectrons. Φ stands for the work function of the spectrometer which is the necessary energy needed to move an electron from the Fermi level of the system into vacuum.

The energy of the photoelectrons leaving the sample is determined by the help of the analyzer which gives a spectrum with a series of photoelectron peaks. Binding energies of these photoelectron peaks are characteristic of elements, thus gives chemical and physical information about the few outer atomic layers of the sample due to the so-called photoelectric effect.[62]

Surface sensitivity originates from the strong inelastic collisions between the generated photoelectrons and the other atoms in the solid. The probe length of XPS is directed by a material dependent value called attenuation length (AL) or inelastic

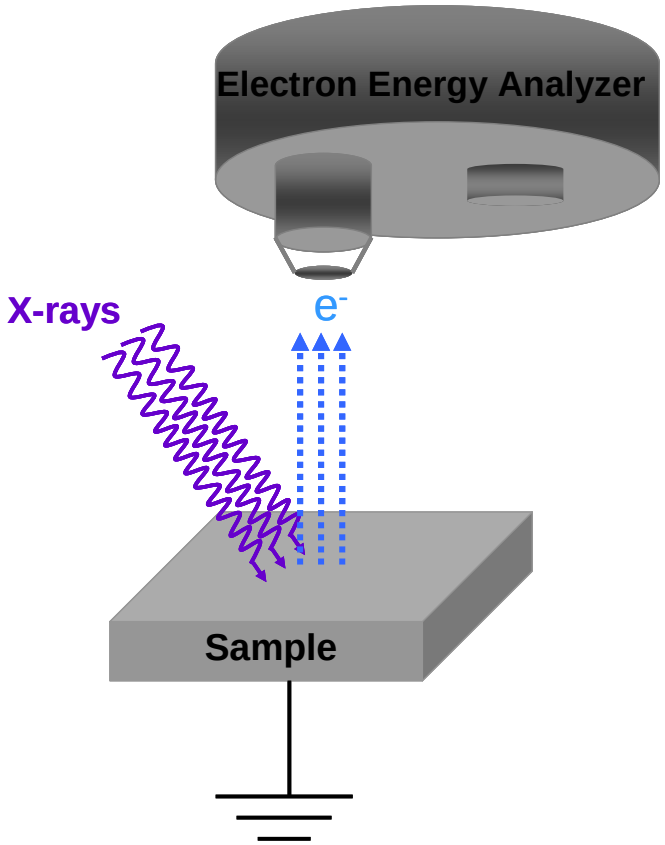

Figure 4. Schematic representation of a typical XPS set-up.

mean free path (IMFP) represented by 'λ'. The term is defined as the distance travelled by the photoelectrons without losing energy while its intensity is reduced to the value of 1/e. The incident photoelectrons lose their energy because of elastic and inelastic collisions. The initial intensity of the photoelectrons, I_o, decays as a function of the distance travelled into the solid according to the relationship, which is defined as:

$$I/I_o = e^{-d/\lambda} \quad (2)$$

The short range of the probe length, 10-20 nm, has very important consequences especially for the nano-sized structures through its high surface sensitivity. Additionally, the surface sensitivity can also be increased by changing the analyzing angle of the emitted electrons with respect to surface plane of the sample

as illustrated in Figure 5. The method is called Angle Resolved XPS where the depth length is decreased down to 1-2 nm.[63,64]

During XPS measurements, electrons are emitted from the sample under investigation and they flow to the analyzer. As a result of this process, a positive charge is generated on the surface of the sample which is known as 'surface charging'. If the sample is a conductive material, the positive charge can be replenished with an electron withdrawn from the ground. In contrast, if the sample is a poor conductive or not grounded material, positive voltage is created on the surface of the sample with respect to the ground. This leads to a variation in the binding energies in the spectrum. In order to eliminate these charges, sample is usually directed to a flow of low energy electrons.

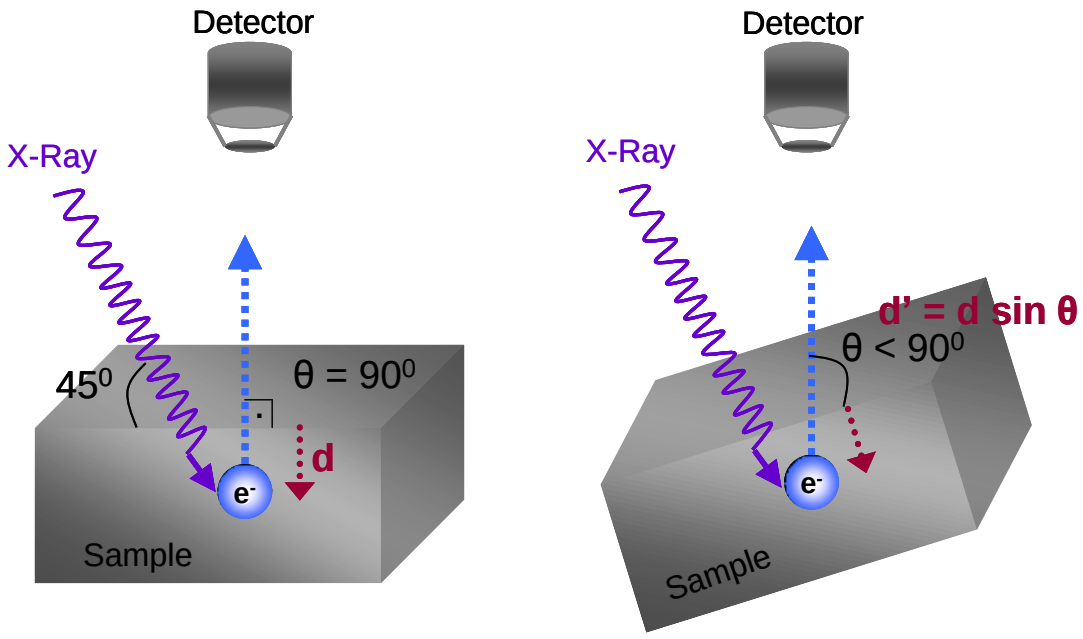

Figure 5. Illustration showing the variation of the depth length as a function of the take-off angle.

However, in some conditions, it may also lead to negative charging because of the excess number of electrons.[63,65] On the other hand, charging of the sample

during photoemission process can be very beneficial in order to extract additional information about the sample under analysis if the extent and sign of the charging can be controlled as reported in literature.[63,66-69] In order to control charging, one of the most versatile method is application of an external bias. For a conductive material, the positions of photoelectron peaks are displaced equally by the application of a voltage stress. However, if the sample is non-conductive, altering in the position of the photoelectron peaks will not be equal, because the charge accumulation is not only dependent on the applied voltage but also on the different capacity of the charge domains. When an external bias is applied to a Si/SiO_2 system, the binding energy difference between Si^{+4} and Si^0 increases under negative voltage stress and decreases under positive voltage stress. Generation of the secondary electrons, stray electrons and the electrons coming from the filament also contribute for neutralization process. In the case of the application of the positive bias, more electrons are attracted to the surface resulting with decreasing binding energy difference between Si^{+4} and Si^0 2p peak. Conversely, under negative bias, these electrons will be repelled from the surface and lead to increase in the binding energy difference.[64]

1.3.2 Applications of XPS in Polyelectrolyte Multilayers

XPS is an important analytical tool for characterizing thin film structures like layer-by-layer deposited polyelectrolyte multilayers, which gives the opportunity to extract useful information such as elemental identification, composition, chemical state and thickness. The binding energy of the peaks is element specific and XPS can identify all elements except hydrogen and helium. In the case of the multilayer structures, the adsorption of each layer can be monitored using XPS.[69] Figure 6

shows a survey XP spectrum of the SiO_2/Si substrate coated by a positively charged polyelectrolyte (Poly(allyamine hydrochloride)) and a negatively charged polyelectrolyte (Poly(styrene sufonate) sodium salt). N1s signal corresponds to PAH where S2p peak is an evidence for the adsorption of the PSS. In most of the layer-by-layer studies, XPS is used for characterization. Lourenço et al. analyzed the influence of NaCl salt on the presence of the counterions in the LbL films.[9]

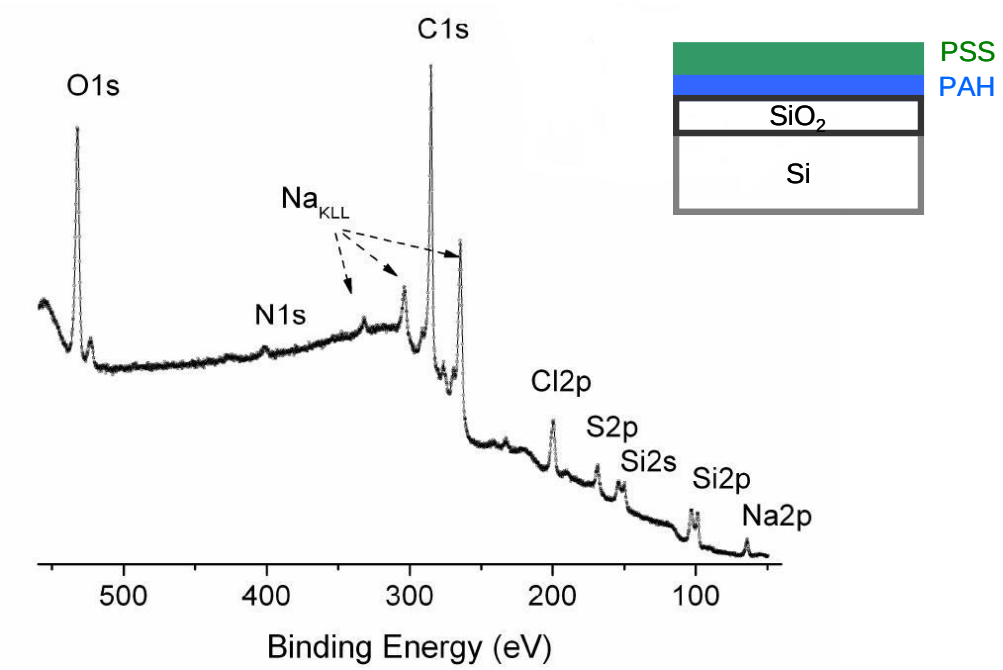

Figure 6. Survey spectrum of a bilayered Si/SiO_2 system.

Oppositely charged polyelectrolyte films were investigated with different ionic strengths using XPS.[9] It was established that when films were washed with pure water after each deposition step, counterions were distributed through the bulk film. Nevertheless, when the films that were washed with salt after each deposition,

part of the counterions were distributed through the bulk film and the other part stayed on the film surface. A detailed work about the dependence of the Donnan potential on the acid-base equilibria in LbL self assembly (LbL-SA) films was reported by Tagliazucchi et al.[70] In order to characterize the films, they combined electrochemical methods such as cyclic voltammetry (CV) and electrochemical quartz microbalance (EQCM), with XPS and Fourier Transform Infrared Reflection-Absorption Spectroscopy (FTIR-RAS). They obtained two independent contributions to the Donnan potential where one arising from the charges that are located in the outer region of the multilayer and the other one produced by the charges that are created or destroyed during protonation or deprotonation of the amino groups. In order to determine the degree of protonation of these amino groups, quantitative analysis was made by XPS and FTIR. Another elemental analysis with XPS for the confirmation of multilayer structures was demonstrated by Liu et al.[71] They presented the usage of LbL process in order to fabricate catalyst particles of a controlled size distribution and packing density for aligned carbon nanotube growth. By using the UV-Vis and X-ray photoelectron spectroscopic measurements, they claimed that LbL process is not only advantageous for controlling the particle size and packing density, but also advantageous for preventing the catalyst nanoparticles from segregation during nanotube growth process.

Besides elemental analysis, XPS is also used in determining the chemical states of the deposited materials in LbL studies. Bruening et al. presented the preparation of catalytic nanoparticle containing films prepared by LbL method.[72] They have also investigated the catalytic selectivity of these films. Alternating deposition of $PdCl_4^{2-}$ and polyethylenimine (PEI) is followed by the reduction of Pd(II) with $NaBH_4$. Formation of the nanoparticles is confirmed with both

Transmission Electron Microscopy (TEM) and XPS. By using XPS, it is determined that ~70% of the Pd in the films was reduced. In the light of this information, they prepared two different systems having different type of polyelectrolytes and number of layers and they determined the effect of overlayers on the turn-over frequencies.

Another important feature of the XPS characterization in polyelectrolytes is that one can determine the thickness of the each adsorbed layer. In a recent work, Caruso et al. presented a detailed work about the thickness determination of polyelectrolyte films on gold. By using proper relationship they found that, a four-layered polyelectrolye film has a thickness about 7.5 nm where reliability of this value was also supported by SPR and UV measurements.[73] Another work for thickness determination of the polyelectrolyte films is presented by us where the average thicknesses of the overlayers were estimated by using the formula for the attenuation of XPS signals.[69] The relationship is further simplified by making measurements in two different take-off angles and the thickness of the each polyelectrolyte layer is estimated as 0.6 nm.

The quantitative analysis can also be made in XPS experiments by using the area of the monitored peaks. Hsieh et al. reported for the multilayer assemblies of PSS and PAH that are formed by sequential adsorption, XPS can be used to determine the stoichiometry between ammonium ions and sulfonate groups.[74] It has been shown that the stoichiometry has differed from substrate to substrate and this information can be utilized to determine a general method for polymer surface modification.

1.4 AIM OF THE STUDY

This thesis mainly focuses on the preparation and the characterization of the layer-by-layer assembled polyelectrolyte multilayers and polyelectrolyte/metal nanoparticle films.

In the first part, formation of the polyelectrolyte layers will be presented. This part includes the characterization of polyelectrolyte coated thin films on Si/SiO_2 system with X-ray photoelectron spectroscopy (XPS). Investigation of the response of polyelectrolyte layers to an external stimulus during XPS measurements will also be discussed in detail.

The second part of the study discusses the formation of the polyelectrolyte/metal nanoparticle (Au and/or Ag) films on glass surfaces. The optical properties of these films are investigated with UV-vis absorption spectroscopy and results will be discussed extensively.

The last part presents introducing Au and/or Ag ions into polyelectrolyte films through ion-exchange chemistry. This section will introduce characterization of these films with UV-vis spectroscopy after irradiation with UV light and investigating their in-situ reduction while recording XPS data.

2. EXPERIMENTAL SECTION

2.1 Materials

Poly(allylamine hydrochloride) (PAH), Poly(sodium 4-styrene-sulfonate) (PSS), Poly(ethylenimine) (PEI), Gold(III) chloride trihydrate ($HAuCl_4.3H_2O$), sodium citrate dihydrate ($HOC(COONa)(CH_3COONa)_2.2H_2O$) were purchased from Aldrich. Sodium chloride (NaCl), Hydrochloric acid (HCl), Hydrofluoric acid (HF) and Potassium Cyanide (KCN) were purchased from Merck, Silver nitrate ($AgNO_3$) was from Fluka and $NaBH_4$ from BDH chemicals. Milli-Q Grade water was used in all preparations.

2.2 Instrumentations

In order to record the XPS data, two different spectrometers KRATOS ES300 and ES800 with MgKα (not monochromatized) sources at 1253.6 eV were used. All measurements were done with a base pressure of 10^{-8} Torr. Sample is subjected to the X-rays with a 45^0 angle and the analyzer is located on top of the sample with a 90^0 with respect to the surface of the sample plane where in this orientation the take-off angle is 90^0, unless otherwise mentioned. The sample rod is connected to either the ground or a DC power supply externally while recording the XPS data under external bias. An illustrative XPS measurement under DC external bias is represented in Figure 7.

Double beam Varian Cary 5E spectrophotometer was used for UV-Vis absorption measurements.

For contact angle measurements, Tantec Contact Angle Meter was used.

254 nm deep UV radiation using a low-pressure 10 W Hg lamp was used to irradiate samples containing ionic gold.

The Scanning Electron Microscope (SEM) image was recorded using ZEISS EVO-40. The image was recorded at 5.00 kV (EHT) operating voltage and at 1.90 A filament current.

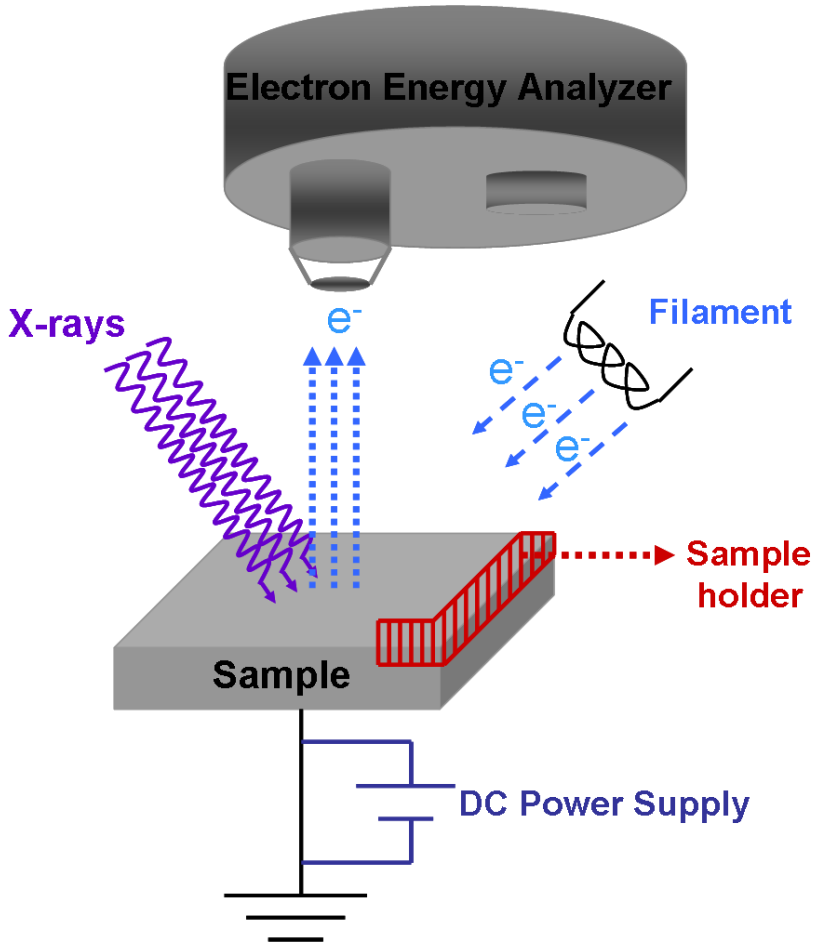

Figure 7. Schematic diagram of a DC biased XPS set-up.

2.3 Procedures

2.3.1 Preparation of Polyelectrolyte Multilayers on Silicon Surfaces

For this purpose, cationic type polyelectrolyte poly(allylamine) hydrochloride (PAH) and anionic type polyelectrolyte poly(sodium 4-styrenesulfonate) (PSS) were used. Adsorption procedure was carried out from 0.15M NaCl solution with an

amount of 0.5 g/l polyelectrolyte, using established procedure.[1,3] Because PAH is a weak electrolyte, having strong structural dependence on pH, the pH of the solution was adjusted to 8.0. As a support material, HF-cleaned Si (100) substrate was used with further thermal treatment at 700 °C in air to grow a thin oxide layer. The substrate was first dipped into the 0.10 M NaOH solution. Deposition was performed by further dipping into the separate PAH and PSS solutions respectively. Samples were rinsed with deionized water for 1 min after adsorption of each layer. By dipping the samples into polyelectrolyte solutions in an alternative fashion, one can build-up as many layers as needed.

2.3.2 Preparation of Polyelectrolyte/Metal Nanoparticle (Au and/or Ag) Films

Polyelectrolyte/metal nanoparticle films are prepared in the same manner with the polyelectrolyte multilayers. Glass or quartz are used as the support materials. The substrates are treated with 0.01M NaOH solution first about 40 min. cationic type polyelectrolyte, PAH, is used for the deposition partners of the citrate-capped nanoparticles since the citrate capping renders the nanoparticle a negative charge. The deposition process starts with PAH (0.5 g/l) for 1 hour. The adsorption is followed with dipping the supporting substrate into nanoparticle solutions that are in the same concentration as they were prepared. Alternating deposition of glass or quartz into polyelectrolyte and nanoparticle solutions gives multilayer structures.

2.3.2.1 Preparation of Citrate-Capped Gold Nanoparticles

0.5 mM Tetracholoroauric acid salt was dissolved in 100 ml water and heated to boiling temperature under vigorous stirring. Preheated (~ 30^0 C) 5 ml 1 wt % sodium citrate solution was added quickly to the boiling gold solution. The solution is boiled for about 15-20 min. Color change to red wine indicates formation of gold nanoparticles with 15-20 nm avarege size. The UV-Vis absorption spectrum gives a sharp peak at 520 nm.

2.3.2.2 Preparation of Citrate-Capped Silver Nanoparticles

For the preparation of the silver colloids, 0.3 mM 99 ml solution of citrate and 1mM $NaBH_4$ is cooled for about 30 min. 1 ml of the cooled $AgNO_3$ (0.01M) solution is added to the solution under vigorous stirring. $NaBH_4$ is added to the citrate solution just before addition of the $AgNO_3$. The color of the solution turns to yellow which is an indication of the silver colloid formation at around 10 nm. UV-vis absorption spectrum gives a sharp peak at 400nm.

2.3.2.3 Cyanide Treatment for Gold Nanoparticle/Polyelectrolyte Systems

0.01 M KCN was used in all treatments. The films were prepared as explained above. In order to etch gold, corresponding films were inserted into the KCN solution for about 30 seconds and washed with deionized water about 1 min after each dipping. UV-Vis spectrum was recorded after each and every KCN treatment.

2.3.3 Incorporation of Au Ions into Polyelectrolyte Multilayers and their In-situ Photochemical Reduction

Typical polyelectrolytes, PEI, PSS and PAH are employed for building up multilayers before introducing Au ions. As a supporting material, glass is used that is pretreated with Piranha solution for 40 min. PEI (1mg/ml) is used as a first layer and each polyelectrolyte layer adsorption has lasted 1 h and followed with 1min washing. After the deposition of the PEI, the substrate is dipped into PSS (1mg/l) and PAH (1mg/l) solutions respectively, both involving 0.75M NaCl. In the case of the introducing Au ions, the outermost layer should be PAH having Cl^- as counterions. Deposition time for the Au ions is chosen as 12 h. Additional polyelectrolyte layers can also be deposited on top of the metallic layers by using the same procedure.

After the integration of the Au ions, the films are exposed to 254 nm deep UV radiation using a low-pressure 10 W Hg lamp to induce the reduction of Au in the polyelectrolyte matrix. The reduction of the ions and subsequent nanoparticle formation were followed by Cary 5E UV-vis-NIR spectrometer which will be discussed in detail.

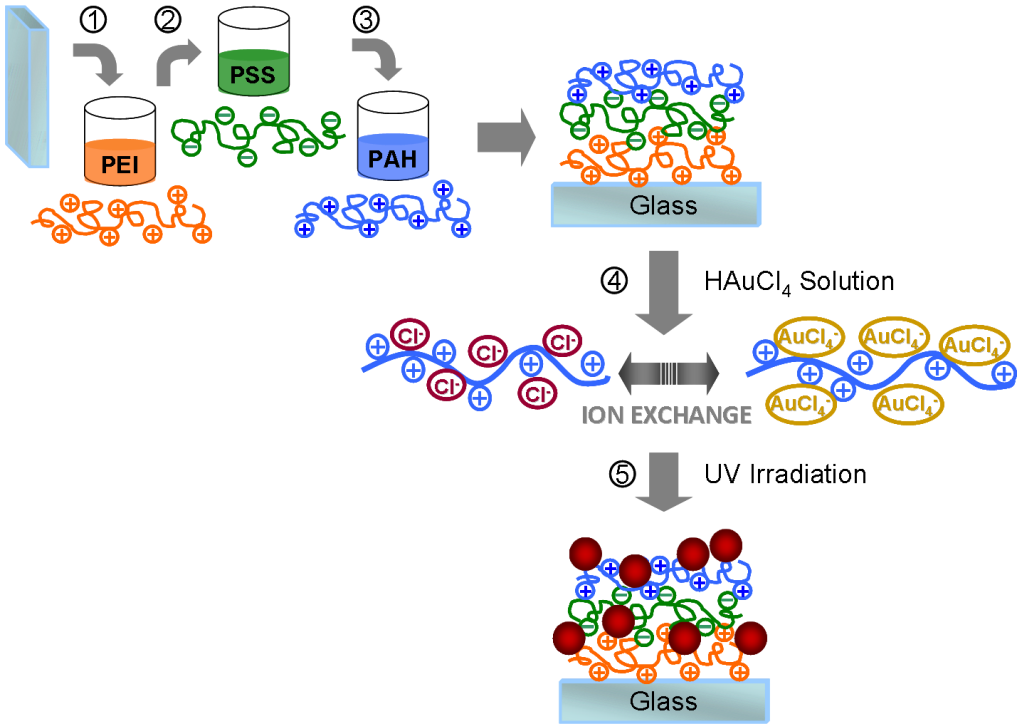

Figure 8. Schematic representation for introducing the Au ions into polyelectrolyte multilayers and their subsequent reduction.

3. RESULTS AND DISCUSSION

3.1 Characterization of Layer-by-Layer Assembled Ultra-Thin Polyelectrolyte Films on Si/SiO_2 Substrate

3.1.1 Water-Contact-Angle Measurements

Sequential adsorption of oppositely charged polyelectrolyte layers results with different wetting characteristics. The traditional method for assessing wetting properties of heterogeneous surfaces is the Water Contact Angle (WCA) method. For an alternately deposited PAH and PSS layers, contact angle measurements show that wetting characteristics of the supporting surface changes through hydrophobic to hydrophilic after each polyelectrolyte insertion. In Figure 9 it is shown that, the average contact angle for a PAH-terminated surface is about 70º, and for a PSS-terminated surface, it is observed to be around 40º. The periodicity of the change in the contact angle is reserved even for multiple layers, so one can easily follow up and ensure the deposition of a polyelectrolyte layer by the WCA measurements.

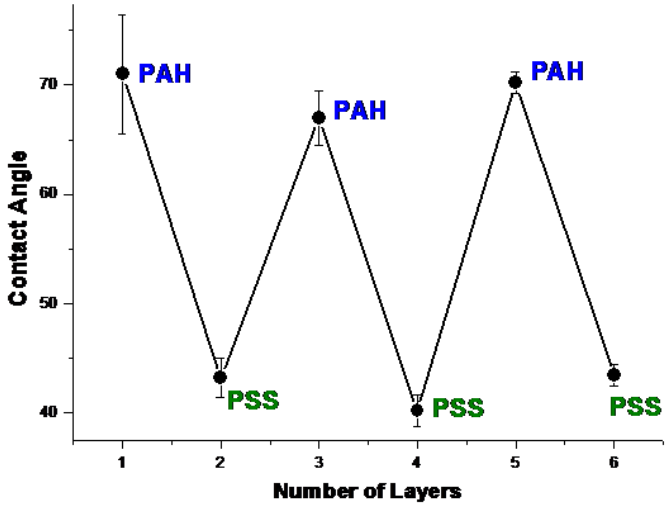

Figure 9. Water-Contact-Angle measurements after deposition of each PAH/PSS layers.

Although water contact angle method is used for evaluating the wetting properties of the surfaces, it gives information only on the macroscopic level. Because controlling the surface properties of the surfaces is still a great challenge for most of the scientists, for more detailed information in the molecular level, various other types of spectroscopic and imaging methods are utilized. Due to the chemical specificity and interface sensitivity, XPS is one of the most powerful techniques for extracting molecular information.[61,75,76]

3.1.2 XPS Characterization of Single Layered Polyelectrolyte Film on Si/SiO_2 Substrate

In surface analysis, XPS is one of the most powerful techniques because of its high surface sensitivity (1-20 nm).[61] By using XPS as a characterization tool, one has a chance to extract useful and unique information such as elemental identification, composition, chemical state of the surface species and thickness.

As discussed in the experimental part, in XPS analysis if the sample under investigation is a non-conductive material, it may lead to positive charging due to the photoelectrons emitted from the sample. By using direct flow of low-energy electrons, one can prevent the material from these charges, where under some conditions it may also lead to negative charging due to capture of excess electrons.[63,65] Applying an external voltage bias can control this surface charging and provide further analytical and electrical information.[66-68,77-83] In order to extract additional information for the polyelectrolyte films, the same approach can also be used.

A single layer polyelectrolyte film is prepared on silicon with ca. 5 nm oxide layer on top and investigated with XPS as shown in Figure 10. For Si/SiO_2 system

with an additional PAH overlayer, an external -10V and +10V potential is also applied, respectively during XPS measurements. The reason for applying a negative bias first is to ensure that the oxide layer is positively charged which is evidenced by a measured binding energy 104.6 eV for of $Si2p^{4+}$ peak. For a silicon substrate the Si2p binding energies is 99.5eV and for a truly uncharged oxide layer it is 103.2 eV.[15,69] Therefore, a measured binding energy larger than 103.2 eV corresponds to a positively charged oxide layer, and similarly for the smaller values, the oxide layer is negatively charged. After applying a negative voltage, the polarity is switched to positive in order to obtain a negatively charged oxide layer which is again evidenced by a measured value of 102.9 eV. When the polarity is switched from negative to positive, the peak positions of the corresponding atoms shift but there is no change in the total intensity ratio of oxide and the silicon substrate peaks. The shift in the composite C1s peak is 2.3 eV which is slightly larger than the shift in the oxide peak (1.7 eV), and there is no change in the total intensity upon switching the sign of the applied potential. But in the case of the N1s peak corresponding to PAH, the situation differs. In order to follow the chemical changes more in detail, the composite N1s peak is curve-fitted into two components, where one of them corresponds to neutral $–NH_2$ and the other one to the quaternized $–NH_3^+$, which is located at ca. 1.5 eV higher binding energy than neutral $-NH_2$[84] and both of them shift by switching the polarity of this bias.

The measured binding energy shifts make possible to determine the potential developed under -10 and +10 V bias both in the oxide and the PAH layer which is shown schematically in Figure 11. The oxide and the PAH overlayer do not respond to the full -10.0 eV shift under negative bias because of the positive charge build-up. They exhibit +1.3 and +1.6 eV average charging shifts respectively and they remain

at the level of -8.7 and -8.4 eV. Similarly under the positive bias, the respond is not full to the +10.0 eV shift but they are at +9.6 (-0.4eV shift) for the SiO_2 and +9.3 (-0.7 eV shift) for PAH layers.

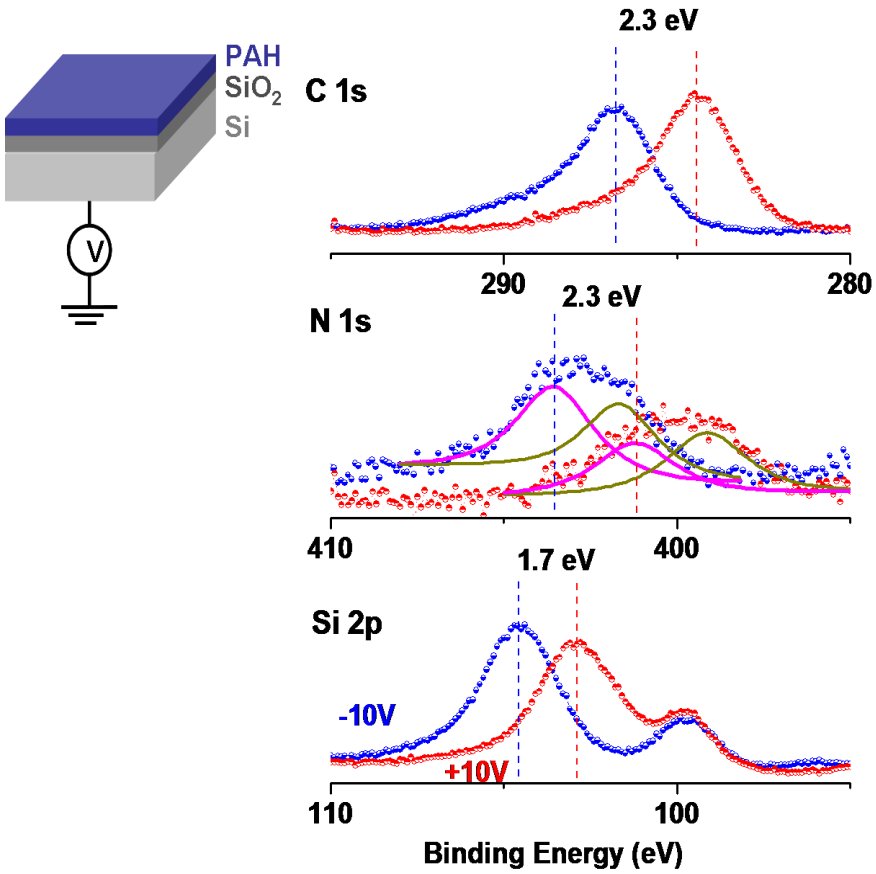

Figure 10. XP spectrum of a single polyelectrolyte (PAH) on Si/SiO_2 substrate recorded under -10 V and +10 V external bias.

For self-assembled mono and multilayers, charge sensitive measurements by XPS have been reported in the literature. It was claimed that, for a single monolayer of a self-assembled alkylphosphonate film, no charging shift was observed. They also stated that only for a multilayer film, a measurable charging shift could be observed.[68,80] Maidul Islam et al. reported a similar contribution for Langmuir-

Blodgett films[85], where for a single LB film no differential charging was recorded but in the case of multilayers, considerable charging shifts were observed.

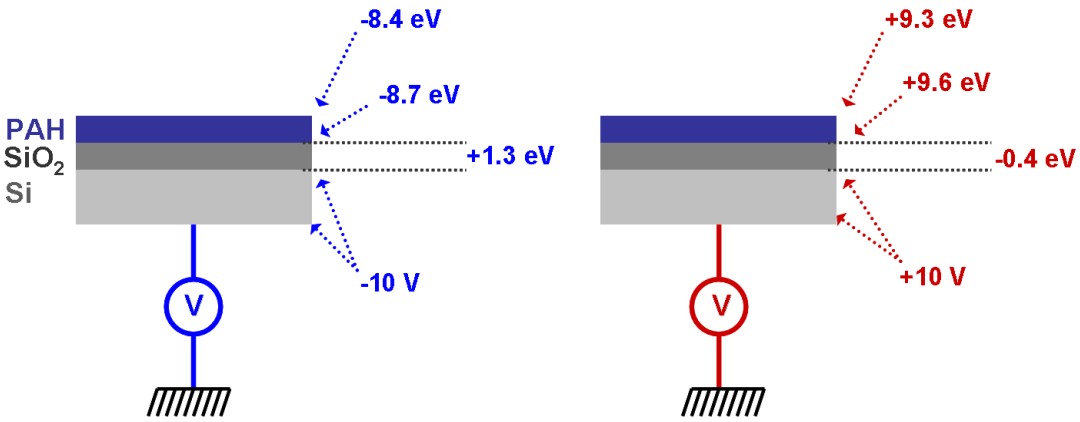

Figure 11. Schematic representation of the measured potentials by XPS when the sample is under (a) -10 V and (b) +10 V external bias.

Conversely, a recent work by Cohen et al. reported that charging effects in different chemical moieties can be recorded down to sub-monolayers.[86] In the case of our experiments, the angle dependent XPS measurements show that, the thickness of a polyelectrolyte layer is about 0.6 nm, where our finding is somewhere in between those reported.

Besides the observed charging shifts in the N1s peak, there is also a change in the overall intensity upon switching the polarity in contrast to Si2p and C1s peaks. The curve fitted peaks enable us to determine the intensity changes in the neutral –NH_2 and positively charged –NH_3^+ peak separately. It is observed that there is almost no intensity change for the uncharged –NH_2 peak, where a significant alteration is observed for positively charged quaternary –NH_3^+ peak, ca. 30 % when the sign of the potential is changed (Figure 12).

We attribute this intensity change to the reorientation of the positively charged groups on the polyelectrolyte overlayer upon switching the charge of the

oxide layer. As it is also depicted in Figure 13, when the oxide layer is negatively charged, the positively charged groups rearrange themselves toward the oppositely

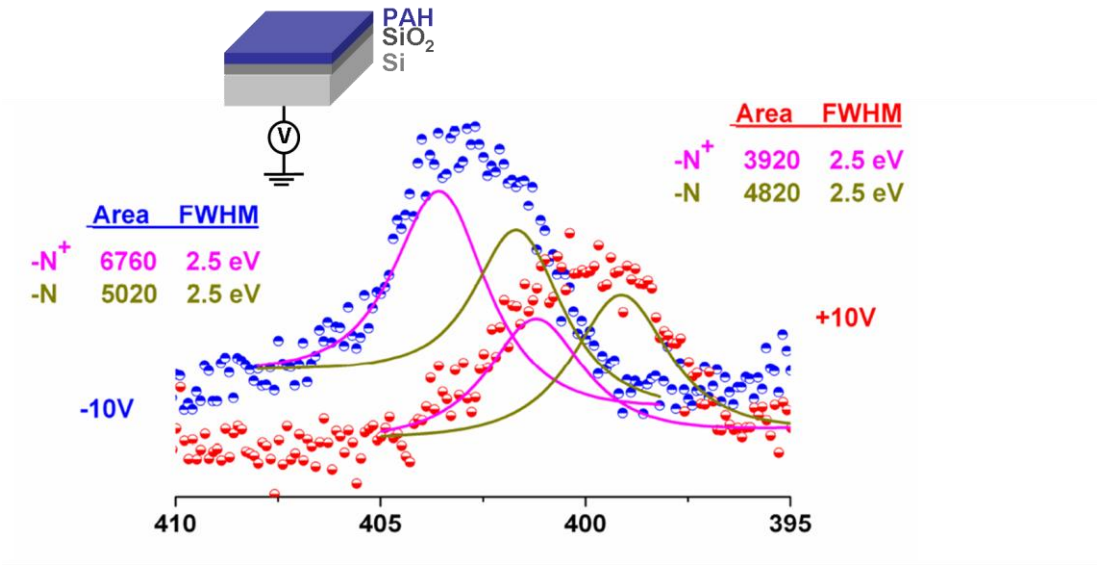

Figure 12. The curve-fitted N1s region with two components ($-N^+$), (-N) and their corresponding areas in units of total counts and full-width-half-maximum (FWHM) values in eV under negative and positive external bias for single PAH layer.

charged oxide layer away from the outermost surface. Conversely, in the case of the positively charged oxide layer, ammonium groups move to the outermost layer because of the repulsive forces between them. A similar chemical respond to an electrical stimulus for low-density monolayers through conformational reorientations was reported by Lahann et al.[87] They demonstrated that interfacial properties of the single-layered molecules can be controlled dynamically. Upon applying an electrical potential, they observed that surface-confined molecules showed change in wetting behavior due to the conformational transitions from a hydrophilic to a moderately hydrophobic state. The transitions were confirmed in both molecular and macroscopic level by the use of Sum-Frequency Generation Spectroscopy and Water Contact Angle measurements, respectively.

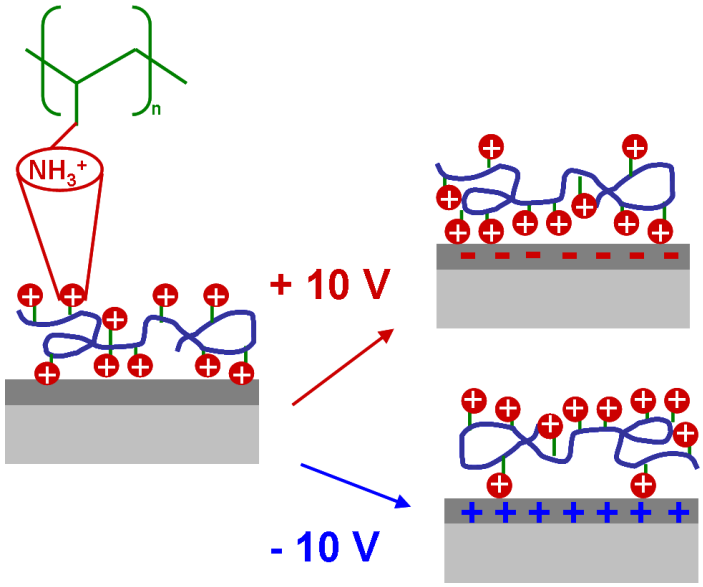

Figure 13. Schematic representation of the rearrangement of the positively charged ammonium groups upon switching the sign of the potential of the substrate from -10V to +10V.

3.1.3 Angle Dependent XPS Characterization of Single Layered Polyelectrolyte Film on Si/SiO_2 Substrate

As it is discussed in the introduction part, angle dependent XPS measurements can be used for estimating the average thickness of the adsorbed polyelectrolyte overlayers. For a uniform overlayer with a thickness d, intensity of the substrate signal is attenuated due to a well-known formula:[69]

$$I_s / I_s^0 = \exp(-d / \lambda_s * \sin\theta) \quad (3)$$

where I_s and I_s^0 correspond to the intensity of the substrate signal with and without an overlayer, respectively, λ_s to attenuation length inside the overlayer and θ to the electron take-off angle. By making the measurements at two different take-off angles, the equation can be further simplified as:

$$[I_s^{30} / Is^0 = \exp (- d/ \lambda_s * \sin 30)] / [I_s^{90} / I_s^0 = \exp (- d/ \lambda_s * \sin 90)] \quad (4)$$

By taking $\sin 30^0 = 0.5$ and $\sin 90^0 = 1$, the equation (4) simplifies to:

$$I_s^{30} / Is^{90} = \exp (-d / \lambda_s) \quad (5)$$

Therefore, the thickness of the overlayer can be predicted by simply taking the intensity ratio of the substrate peak, i.e. the ratio of the area of the Si^{4+} peak at 30^0 to the intensity at the 90^0, if λ_s is known. The attenuation length can be estimated as 3.4 nm, from the measured for a self-assembled thiol monolayers by Main and Whitesides[88] at the kinetic energy of the Si2p peak. The experimentally determined intensity ratio of the Si2p peak of oxide at 30^0 to 90^0 which is also shown in Figure 14 is 0.84 having a single PAH overlayer. By inserting this ratio into the equation (5) leads to estimation of the thickness of the PAH layer.

$$\ln [I_s^{30} / I_s^{90}] = (- d / 3.4) = \ln (0.84) = - 0.174 \rightarrow d = 0.6 \text{ nm}$$

The same thickness value for a single PAH layer was also determined by Caruso et al., using SPR and QCM techniques.[73] In the case of SPR measurements, the thickness was determined as 0.6 nm and 0.5 nm by using QCM method. XPS was also used for calculating the thickness of four polyelectrolyte layers and the thicknesses were determined as 7.5 nm and 8.5 nm in independent experiments. Similarly, Ramsden et al. calculated the thickness of a single PAH layer on a MPA-

modified gold surface as 0.5 nm by using a planar optical wave guide system.[16] Hence, our value is highly consistent with those reported.

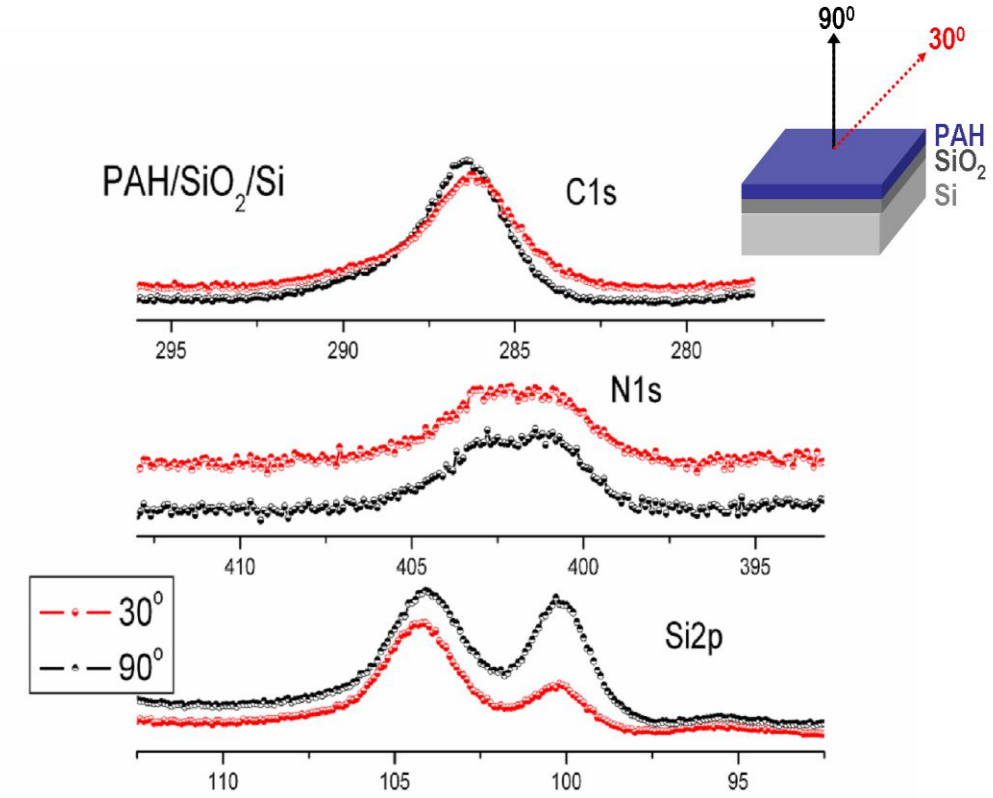

Figure 14. XP spectrum of a single polyelectrolyte (PAH) layer deposited Si/SiO_2 sample showing the regions of C1s, N1s and Si2p, recorded at 90^0 and 30^0 electron take-off angle.

3.1.4 XPS Characterization of Bilayered Polyelectrolyte Film on Si/SiO_2 Substrate

A bilayered polyelectrolyte film can be prepared by the alternating deposition of oppositely charged PAH and PSS layers on Si/SiO_2 substrate as explained in the experimental part. When this sample is characterized with XPS, the situation somehow differs from the single polyelectrolyte layer deposited on Si/SiO_2 film by means of the intensity changes. When PSS is deposited as an additional polyelectrolyte layer on the substrate, having a PAH overlayer, again the same

charging behaviors are observed in C1s, N1s and S2p peaks, but this time without any intensity alteration in N1s peak as depicted in Figure 15 and Figure 16 in detail.

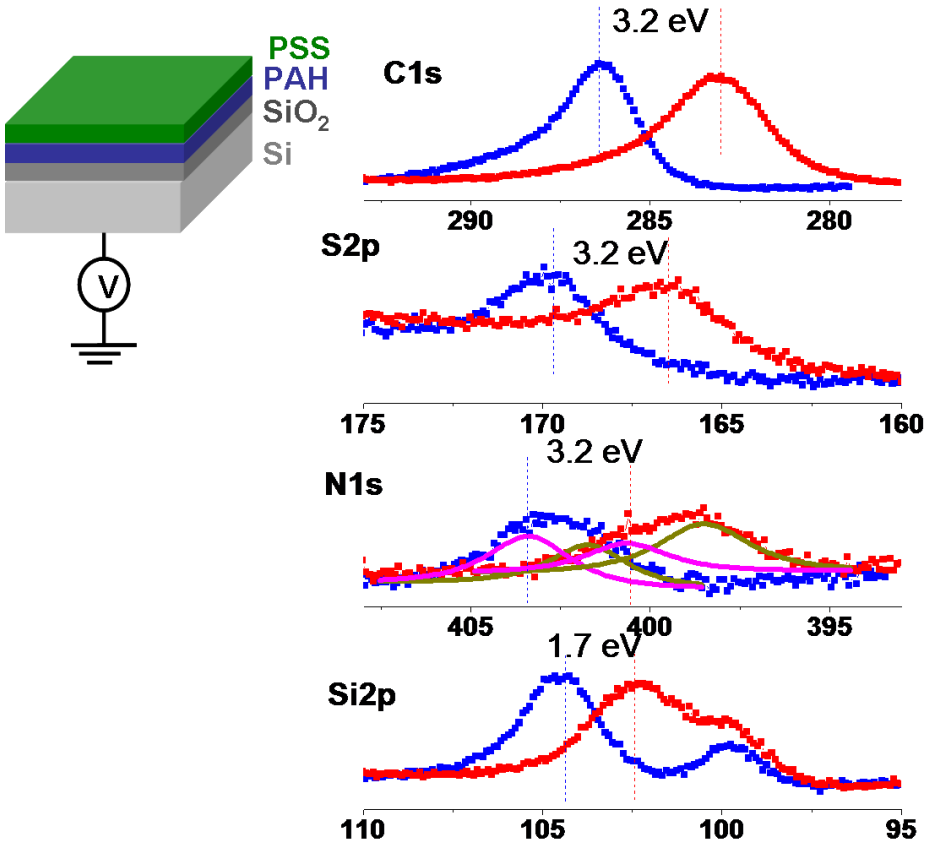

Figure 15. XP spectrum of a single PAH and a single PSS layers on Si/SiO_2 substrate recorded under -10 V and +10 V external.

We explain this behavior to be originating from locking of the positively charged $–NH_3^+$ groups by the negatively charged – SO_3^- groups. When PSS is deposited onto PAH overlayer, the positively charged quaternary ammonium groups can not respond to the change in the electrical stimuli, as explained in Figure 13, because these groups had already interacted with the negatively charged $–SO_3^-$ groups.

3.1.5 Angle Dependent XPS Characterization of Bilayered Polyelectrolyte Film on Si/SiO_2 Substrate

A bilayered polyelectrolyte film is also characterized by angle-dependent XPS measurements. When an additional polyelectrolyte is deposited onto a oppositely charged polyelectrolyte layer, one can ensure the order of the layers deposited by following the decrease in the peak intensities at low electron take-off angles.

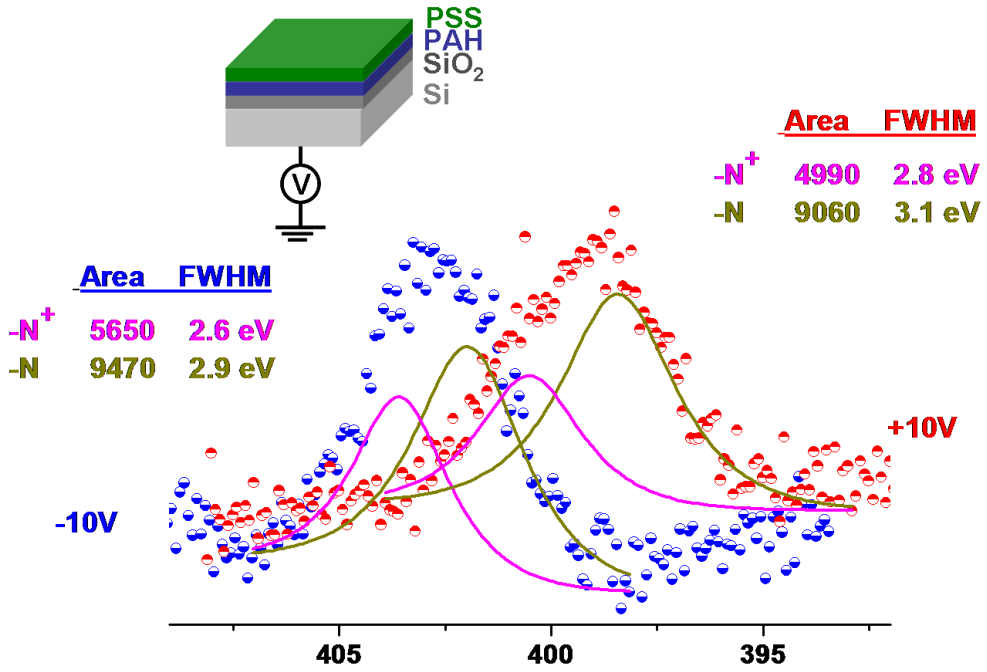

Figure 16. The curve-fitted N1s region with two components ($-N^+$), (-N) and their corresponding areas in units of total counts and full-width-half-maximum (FWHM) values in eV under negative and positive external bias for single PAH + single PSS layer.

In Figure 17 it is shown that, N1s, Si^{4+} and the Si^0 peak intensities decrease upon changing the take-off angle to 30^0 where there is little or almost no change in the C1s peak. When the take-off angle is tilted from 90^0 to 30^0, the surface sensitivity is enhanced and relative intensity of the outermost layer increases. Hence, it is

expected that the alteration in the intensity should be in the order of the N1s, Si^{4+} and Si^{0}. The results follow the expected trend for both single and bilayered polyelectrolyte films on Si/SiO_2 substrate.

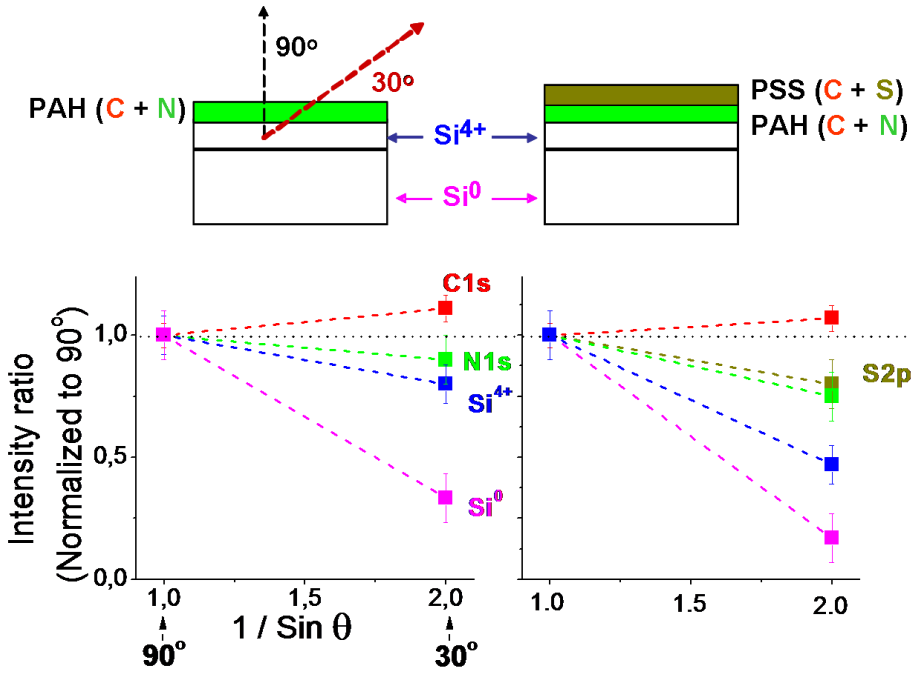

Figure 17. Intensity ratios of the corresponding peaks at 900 and 300 electron take-off angles plotted against 1/sin (electron take-off angle) for one single PAH and one single PAH + one single PSS layers.

Hence, use of XPS in layer-by-layer deposited multilayers has several advantages. Characterizing of these films with XPS gives opportunity to extract useful information such as the elemental identification of the surface elements, surface composition. As shown in our experiments, one can also use Angle-Resolved XPS to determine thickness of the deposited polyelectrolyte layers. In addition, our experimental findings showed that applying an external voltage bias to the sample leads to observe a chemical specific response to an electrical stimulus as evidenced by the recorded data.

3.2 Optical Response of Metal Nanoparticle Incorporated Polyelectrolyte Multilayers

Layer-by-layer deposition is one of the most widely used methods for preparation of nanoparticle containing thin films. The two main aims of this part of the thesis are to prepare multilayer films containing gold nanoparticles and polyelectrolytes utilizing from LbL assembly process and understand their optical properties in compact film structures. Within this purpose, firstly we have prepared a thin film structure having six nanoparticle layers in between PAH layers. Optical spectra revealed that after deposition of the second layer, a new band appeared besides the characteristic SPR band of gold (Figure 18). In order to get better understandings of this interesting optical behavior, we have followed three major experimental approaches; (i) increasing the number of polyelectrolyte layers in between adjacent gold nanoparticle layers to discriminate against the interactions between nanoparticles between adjacent layers, (ii) introducing a different type of metal nanoparticle (Ag) to understand the particle interactions between same and different type of nanoparticles in films, and (iii) etching gold layers selectively with cyanide treatment to reverse the change in the optical responses.

3.2.1 Incorporation of Au Nanoparticles between Polyelectrolyte Layers

When gold and silver nanoparticles are synthesized separately with the Turkevich method, sodium citrate is used as a reducing agent and after the reduction; metal nanoparticles are surrounded by citrate ions which bring out two advantageous; first, because clusters are capped with these ions, they are stabilized in the solution. In other words, particles are prevented from aggregation because of the repulsive forces between them. The other advantage of this capping agent is that it imparts

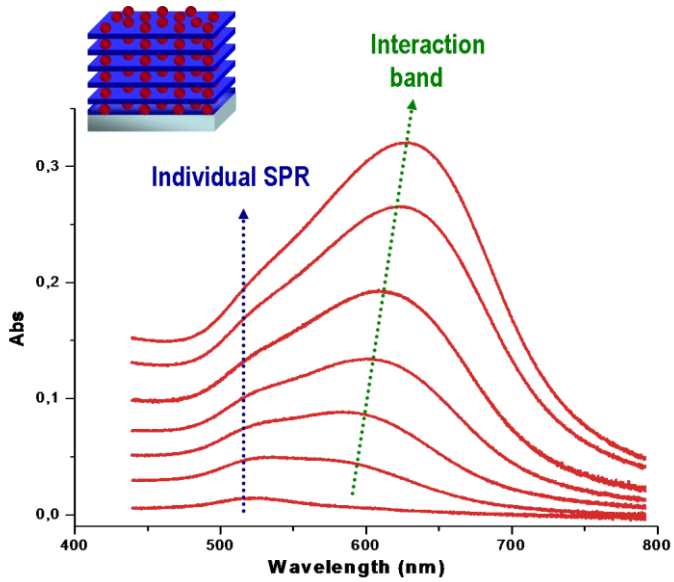

Figure 18. UV-Vis spectra of $(PAH/Au\ NP)_6$ film on a glass surface.

negative charges around nanoparticles to make these nanoparticles suitable candidates for polyelectrolyte assemblies. When cationic type polyelectrolytes are used, citrate-capped nanoparticles can be used as building blocks in the layer-by-layer architecture. Hence, polyelectrolyte/nanoparticle couples are assembled through the same procedure with oppositely charged polyelectrolytes where they are coated on glass surfaces by alternating deposition from their solutions.

When a single layer gold nanoparticle is deposited in between polyelectrolyte layers, it keeps its optical properties as in the solution phase. Figure 19 shows that when gold clusters are sandwiched between PAH layers, the absorption spectrum gives an SPR band around 520 nm, the position of this band is comparable with the solution absorption. It is further observed that there is no additional broadening due to the aggregation, etc.

By using the layer-by-layer approach, one can assemble as many layers as needed by using oppositely charged species. Using this same approach, a gold naoparticle/ polyelectrolyte film was prepared having six metal layers. In the step of gold nanoparticle adsorption, the deposition process was about 30 min each. Figure 20a shows that, as the number of the gold nanoparticles increase, absorption spectrum shows a deviation from its solution case. Already after deposition of the

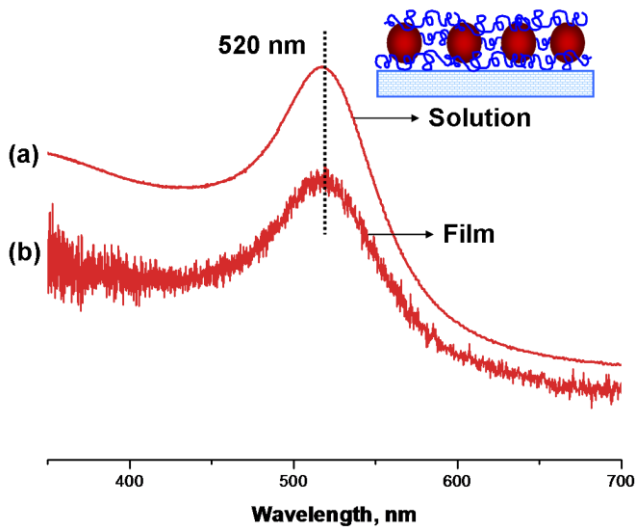

Figure 19. UV-vis absorption spectra of **(a)** gold nanoparticle solution and **(b)** layer-by-layer assembled gold nanoparticle/polyelectrolyte film (PAH/Au NP/PAH).

second gold layer, a new band contributed to the spectrum around 580 nm and red-shifted. This new band's absorption increases much more rapidly than the individual SPR band of the gold. When the areas under both peaks are calculated and plotted against the number of the metallic layers, Figure 20b is obtained. Individual SPR band of the Au nanoparticles shows a linear increase where as the new band follows an exponential trend. This new band is attributed as an interaction between gold nanoparticles either in the same or adjacent layers instead of aggregation of the gold nanoclusters. It has been already known from the literature that when the size of the

gold nanoparticles increases, the plasmon band is red-shifted and broadened without appearance of a new peak.[41] So, the band arising at around 580 nm originates from the interaction between gold nanoparticles in the film.

In a recent work, Tsukruk et al. presented that, for multilayer deposited gold nanoparticle/polyelectrolyte films, there is an additional strong peak besides the characteristic surface plasmon band of gold.[52] They claimed that this strong band is due to the collective resonance from intralayer interparticle coupling which is the interaction between the gold NPs within the same layer. Similar work was also demonstrated by Liz-Marzan's group. Layer-by-layer assembled anisotropic gold nanoparticles in between polyelectrolytes showed a new band around 650 nm and it was ascribed as NP-NP coupling in the adjacent layers.[58]

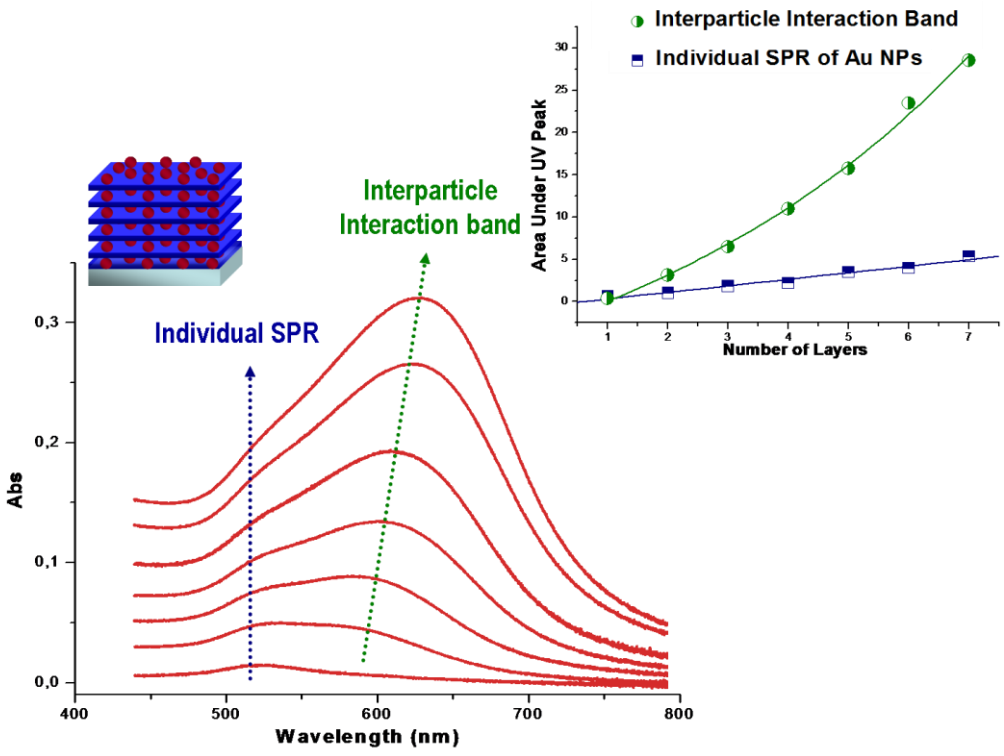

Figure 20. (a) UV-Vis spectra of $(PAH/Au\ NP)_6$ **(b)** Graph showing the relationship between area under UV peak and the number of metal layers.

In order to make a further understanding, we increased the adsorption time of gold in a single layer gold nanoparticles on top of the single PAH layer. Figure 21 shows that, 15 min adsorption times gives a peak around 520 nm. As the deposition time increases, the band broadens and red-shifts but no other new peak is observed. Because number of the gold nanoparticles on the surface increases, there is also an increase in the absorption band. But although the Au concentration increases on the surface, no interaction peak is obtained. It should be noted that, the concentration of the gold solution is kept the same in both multilayer formation experiment and this experiment is performed in order to make a consistent comparison.

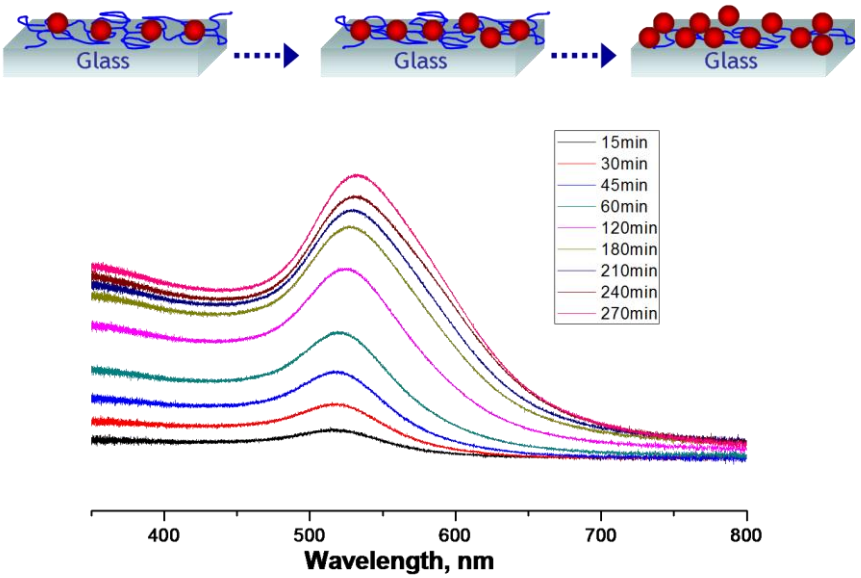

Figure 21. UV-Vis spectra of a one PAH layer + one Au nanoparticle layer with different deposition times.

Inserting more polyelectrolyte layers would create an inert media for controlling the interaction between nanoparticle in adjacent layers. In Figure 22 it is shown that the gold nanoparticle layers were separated through deposition of one, three and five polyelectrolyte layers between them. It was observed that when the

numbers of the polyelectrolyte layers are increased in between the gold layers, the interactions between these layers are prevented. When three or five polyelectrolyte layers were deposited between gold layers, there was no additional contribution to the spectrum except the characteristic SPR band of gold. Therefore, one can control the 'interlayer interaction' between the adjacent nanoparticle layers by separating them through increasing the number of the polyelectrolyte layers in between.

Another argument involving the strong band at longer wavelength could be attributed to the fact that gold nanoparticles in the adjacent layers can interact with each other in a different oscillation mode, similar to that gold nanorods. It has been already established in the literature that gold nanorods have two plasmon absorption bands in the visible region, one stands for the longitudinal and the other for transverse mode.[31]

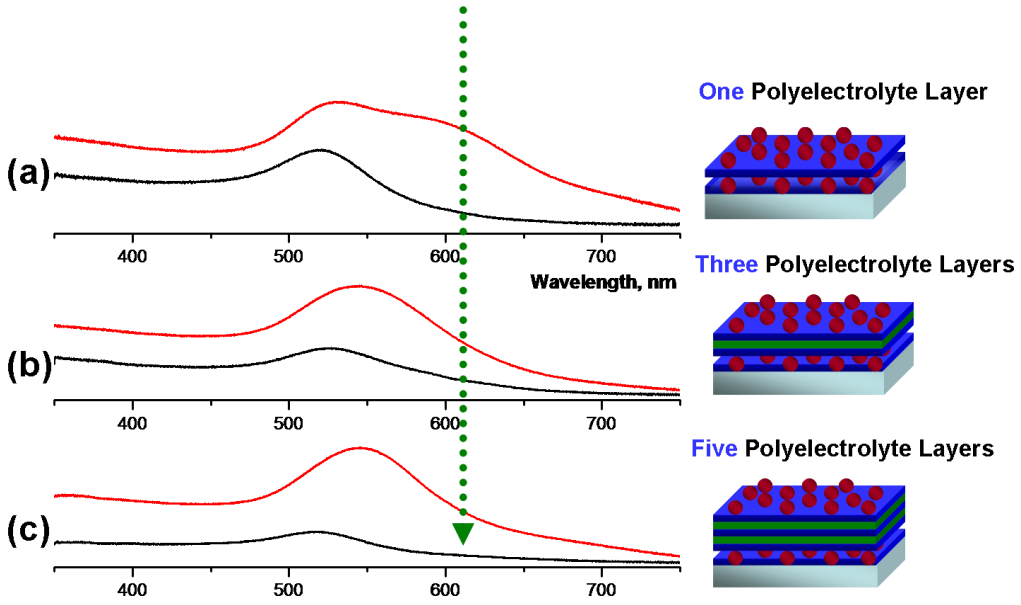

Figure 22. UV-Vis spectra of **(a)** $(PAH/Au)_2$ **(b)** (PAH/Au/PAH/PSS/PAH/Au) **(c)** $(PAH/Au(PAH/PSS)_2PAH/Au)$.

3.2.2 Incorporation of Ag Nanoparticles between Polyelectrolyte Layers

Introducing a different type of a metal nanoparticle into polyelectrolyte layers rather than gold, may give some idea about the interparticle interactions. Therefore we have utilized silver nanoparticles as deposition partners for cationic type polyelectrolytes because of having the same citrate capping. When six-layer silver nanoparticles were deposited between polyelectrolyte layers in a layer-by-layer fashion, it was observed that silver behaves as in the case of gold (Figure 23).

After deposition of the first layer, the SPR band arises around 390 nm. When second layer metal layer is deposited, again a new band contributed to the spectrum. The position of this band was around 505 nm and shifted to longer wavelengths (530 nm) as number of the silver layers increased. When the area under both peaks are curved-fitted and calculated, it has been seen that the both SPR and interaction peak increase linearly as number of the deposited layers increase, but the increase in the interaction peak intensity is much larger than the plasmon band. Although not so strong as in Au case, the interparticle interaction band of Ag is also observable through the polyelectrolyte layers.

3.2.3 Combinations of the Au-Ag Nanoparticles between Polyelectrolyte Layers

One of the most advantageous aspects of the layer-by-layer deposition technique is that one can easily control the sequence of the adsorbed species. By using this property, multilayer films including gold and silver nanoparticles were prepared in different sequences (Figure 24). In Figure 24a it is shown that, silver nanoparticles are used as a first metallic layer, where in Figure 24b, gold nanoparticles are deposited first. In both, there are two separate absorption bands,

one of them corresponds to the SPR band of Ag (390 nm) and the other to that of Au (520 nm).

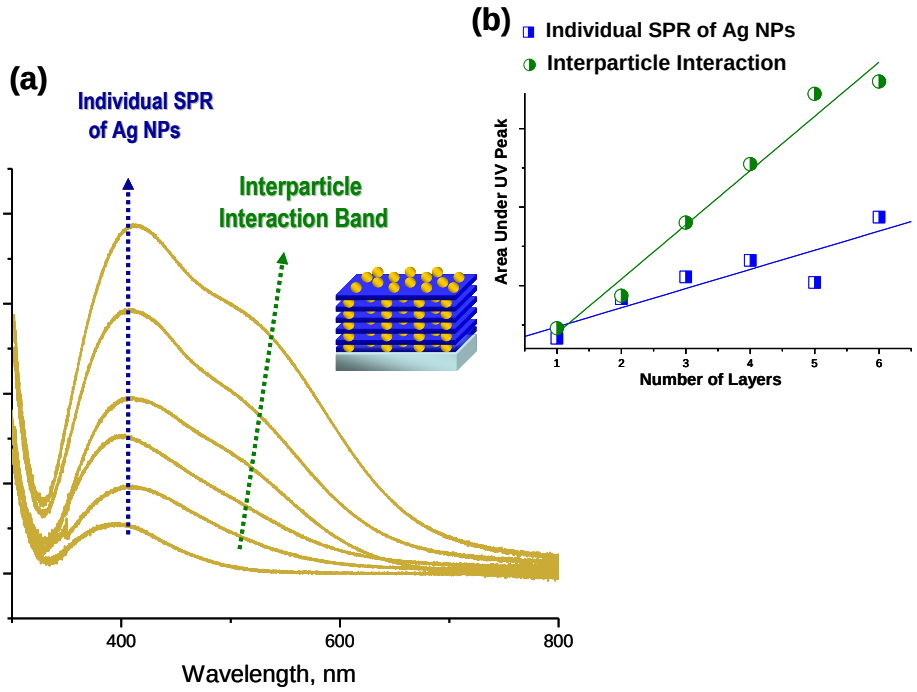

Figure 23. (a) UV-Vis spectra of $(PAH/Ag\ NP)_6$ **(b)** Graph showing the relationship between area under UV peak and number of metal layers.

Two distinct peaks indicate that gold and silver nanoparticles are well-separated. Intensities also give some information about the deposition process. When a different type of metallic layer is coated on the surface, the intensity of the underlying metal layer stays almost constant. Consequently, the relative intensities of gold and silver can be used to check the fate of the deposition process.

In the optical spectra of bimetallic multilayers (Figure 24), interparticle interaction between Ag and Au nanoparticles could not be observed. If there were significant optical interaction between either the same or different type metal nanoparticles, it would be expected to observe an additional plasmon resonance,

possibly between those of Au and Ag. Although, in the separate experiments of gold and silver, a new and strong band appeared after deposition of even after the second metal layer, in the case of multileyers including both metals, no additional contribution was observed after deposition of several metal layers. It is worth to mention that the deposition time, concentration, etc. were identical in single as well as mixed nanoparticle depositions.

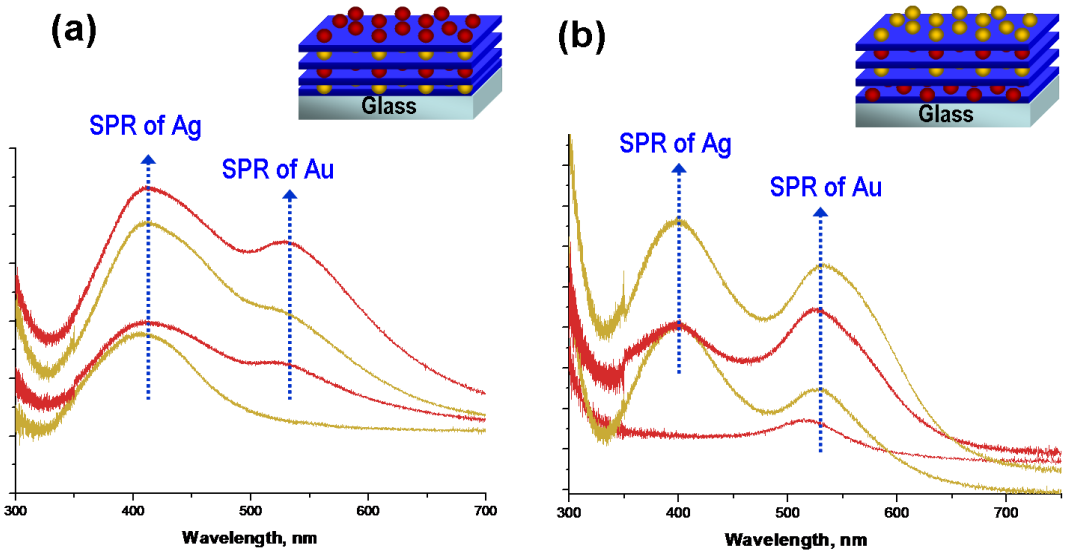

Figure 24. UV-Vis spectra of **(a)** $(PAH/Ag/PAH/Au)_2$ **(b)** $(PAH/Au/PAH/Ag)_2$ film.

3.2.4 Cyanide Treatment for Gold Nanoparticle/Polyelectrolyte Systems

In a recent contribution, Decher et al. presented that fluorescently labeled polymers can be coated on gold colloids by using nonfluorescent polyelectrolytes as spacers.[89] In order to investigate the photophysical behavior of the fluorophores in the presence and the absence of the metal core, the core was treated with cyanide ions. The cyanide treatment resulted with the dissolution of the gold core. By using the same property of cyanide ions, we have tried to subject gold nanoparticle/polyelectrolyte films to cyanide solution treatment in order to remove

gold layers in a controlled way, thereby to get further understanding of the influence of their structural orders and optical properties.

Figure 25 depicts three different gold nanoparticle/polyelectrolyte systems having one, two and three layers on top of the gold layer, respectively, in order to observe the effect of the cyanide treatment on gold with different structural orders. All three systems were treated with cyanide ions for five minutes and again in every 30 seconds UV-vis spectrum was recorded. It is observed that when number of the polymer layers deposited on gold layer is increased, etching of nanoparticles takes longer times. For a three polymer layer deposited system, at the end of five minutes, there is still a significant absorption, although for the first and the second system, absorption is drastically diminished. So, we can conclude that increasing polymer layer on top of gold makes harder the etching process and protects them.

Figure 26 shows a bilayered gold nanoparticle film and a strong absorption corresponding to the interaction plasmon after at the second layer. After preparation of this system, the film was treated with KCN solution. UV-vis spectrum was taken after each 30 seconds and it was observed that intensities both in the SPR band and the interaction band decreases gradually. Because polyelectrolyte layers obstruct the removal of gold, which was also depicted in Figure 25, cyanide ions starts to etch gold nanoparticles from the top. As number of the gold colloids decreased in the upper layer, it would be expected to observe a much rapid decrease in the interlayer interaction band of the Au clusters in the adjacent layers.

When the decrease in the absorbance is plotted against time, Figure 26(c) is obtained. One can easily see that, the absorption decrease in the interaction peak is much more rapid than the SPR band. After one minute from cyanide etching, interaction peak has completely disappeared, where absorption of the SPR band

fades gradually. All of these experimental findings including three major experimental approaches will be summarized in the next paragraph.

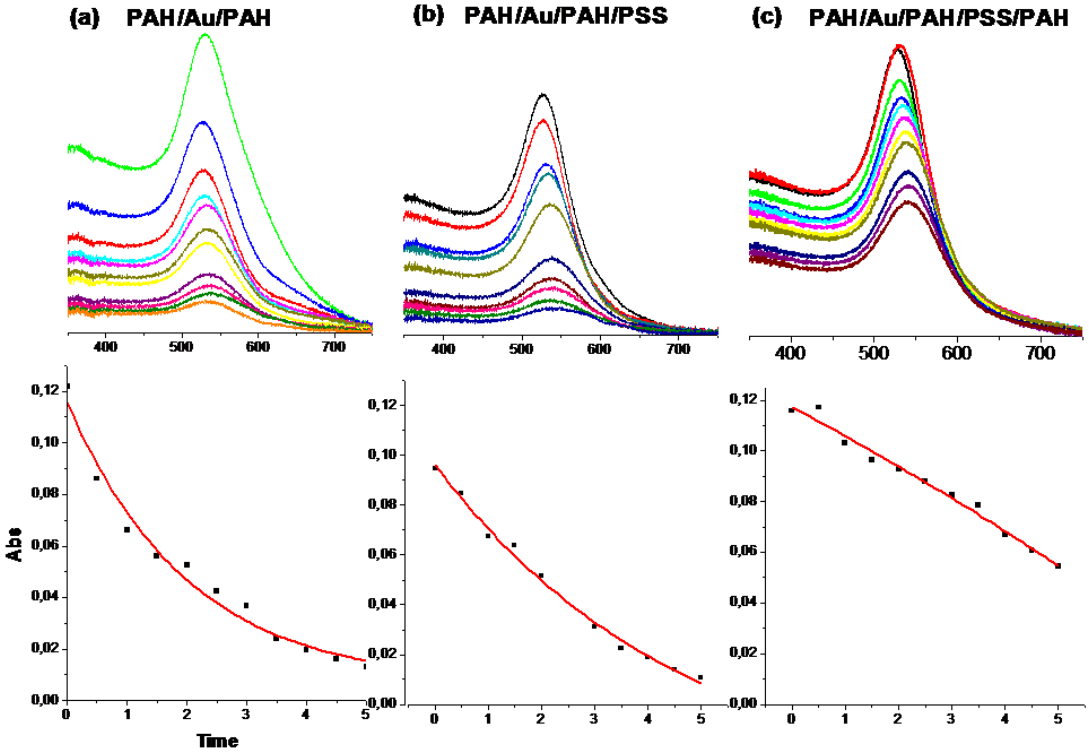

Figure 25. Absorption intensities plotted against time for 0.01 M KCN treated **(a)** (PAH/Au/PAH/PSS) **(b)** (PAH/Au/PAH/PSS/PAH) and **(c)** (PAH/Au/$(PAH/PSS)_2$) films.

As the summary of this section of this thesis, we can state that, by using layer-by-layer assembly process, we have successfully incorporated gold and silver nanoparticles into polyelectrolyte matrices. It was observed that an increase in the number of the deposited metallic layers leads to the formation of the interparticle interaction which is evidenced by an additional contribution in the UV-vis spectra besides the characteristic SPR bands of gold and silver, due to the interparticle interaction through the layers. In order to control and understand this interparticle interaction through the layers, we had followed three simple experimental approaches; (i) by increasing the number of the polyelectrolyte layers between gold

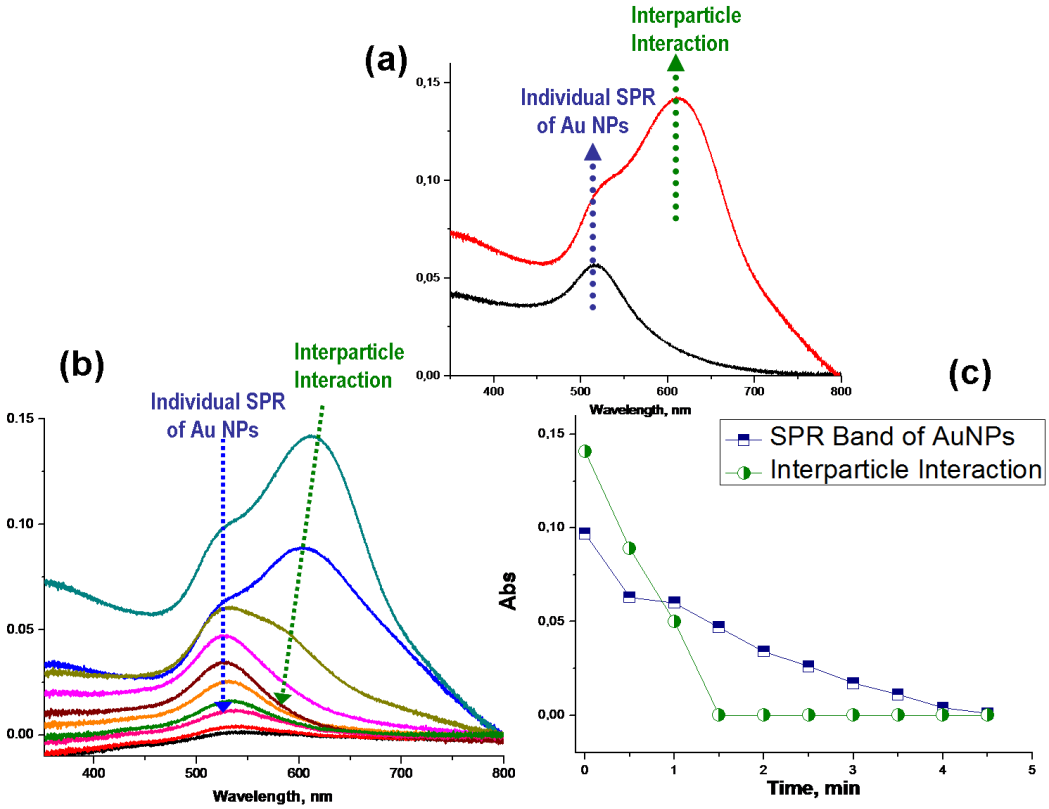

Figure 26. UV-Vis spectra for **(a)** $(PAH/Au)_2$ film and **(b)** 0.01M KCN treated $(PAH/Au)_2$ film **(c)** Absorption intensity plotted against time for a 0.01M KCN treated $(PAH/Au)_2$ films.

layers, we could reduce the interaction of nanoparticles between adjacent layers, (ii) by alternating deposition of different type of metal nanoparticles, we controlled the interparticle interaction where the optical spectra shows only characteristics SPR bands of Au and Ag, and (iii) by treating the films including more than one gold nanoparticle layers with cyanide solution, we could etch the nanoparticles selectively from the outermost metallic layer which leaded to a strong decrease in the interparticle interaction. Therefore, these three experimental approaches independently showed that the band arising with increasing number of the Au layers, originates from the interaction between nanoparticles in the adjacent layers, the so-called 'interlayer interparticle interaction'. By following one of these three

experimental approaches, the interparticle separation and interaction through the metallic layers were controlled and manipulated. The optical properties of the layer-by-layer assembled polyelectrolyte films containing these metal nanoparticles can also be tuned in a controlled way via increasing the interlayer separation, introducing another type of a metal ion or applying a chemical treatment. The absence of the interparticle interaction band in the case of introducing a different type of metal nanoparticle remains as an interesting scientific issue to follow up.

3.3 Incorporation of Au Ions into Polyelectrolyte Layers through Ion-Exchange

Introducing metal ions into a variety of films or matrices leads to unique properties and structures for applications in catalysis, sensing, and/or biochemical areas.[90] In a recent study, Chia et al. presented incorporation of metallic or inorganic ions into multilayer assemblies by creating ionic groups in the multilayer.[29] The desired inorganic salt was introduced by controlling the pH of the solution during fabrication of the thin films from weak polyelectrolytes. Dai and co-workers demonstrated that alternating adsorption of PEI-metal ion (Ag^+) complexes and polyanions yielded formation of multilayered polyelectrolyte films containing metallic ions.[90] In the layer-by-layer assemblies, one can take the advantage of the counterions on the surface of the LbL films by exchanging them with a desired salt where no chemical modification of substrates or polyelectrolytes are needed.[28]

This part of the thesis focuses on two major themes; (i) incorporation of gold ions into LbL assembled polyelectrolyte films, (ii) reduction of the ions under UV-light or X-ray irradiation and their characterization by UV-Visible Spectroscopy and XPS.

3.3.1 Incorporation of Au Ions into LbL Assembled Polyelectrolyte Matrices through Ion-Exchange

Applicability of the ion-exchange method to LbL assembled polyelectrolyte films is based on the nature of the counterions corresponding to the outermost polyelectrolyte layer.[28] As it was expressed schematically in Figure 8, $AuCl_4^-$ ions can be exchanged with Cl^- counterions having PAH as the outermost layer. When the film having PEI, PSS and PAH layers respectively was dipped into an aqueous solution of gold salt, Cl^- counterions in the outermost layer behaves as facilitating hosts for Au ions. The ion-exchange between $AuCl_4^-$ and Cl^- ions is evidenced by using XPS (Figure 27(a)). It has already been established in the literature that counterions located only on the outermost layer and can be exchanged.[91] Because gold has a large photoionization cross section, the exchanged gold ions can be seen clearly in the XPS spectrum.[61] Since, ion-exchange in the layer-by-layer deposited multilayers do not need any chemical modification, after exchanging gold ions, it is also possible to further deposit other polyelectrolyte layers on top. Figure 27(b) shows the XPS spectrum of a sample in which after exchanging gold ions, PAH and PSS layers were deposited on top, respectively. The intensity decrease in the Au4f region is a sign that bilayer polyelectrolyte deposition was indeed achieved.

3.3.2 UV-Induced Reduction of Au Ions in Polyelectrolyte Matrices

Once metallic ions are inserted into a polymeric media, subsequent reduction of metal ions can be carried out in a variety of methods for inducing the important optical, catalytical and magnetic properties of nanoparticles.[29] Post treatment of metal ions incorporated into polymeric matrices yielded nanoclusters via several experimental routes, such as: H_2 exposure,[92] UV[93,94] and X-ray irradiation [30,94,95] and

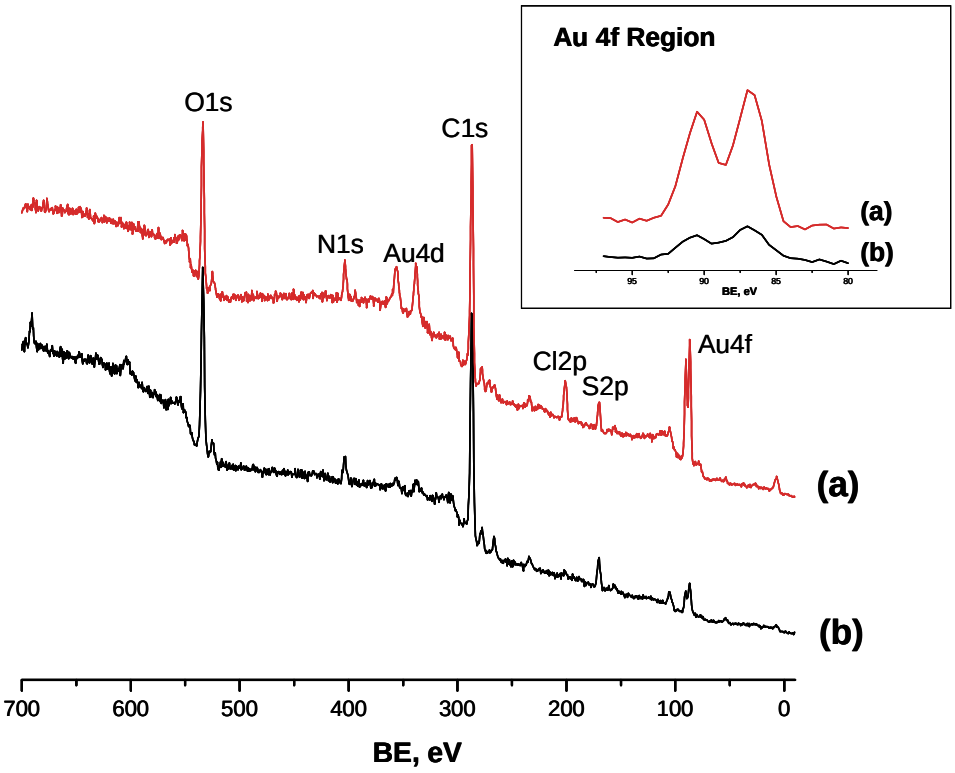

Figure 27. XPS survey spectra of **(a)** $HAuCl_4$ solution treated (PEI/PSS/PAH) film **(b)** $HAuCl_4$ solution treated (PEI/PSS/PAH) film + PAH/PSS.

chemical reduction methods.[29,90,96]

In this part of the study, UV induced reduction of Au ions incorporated polyelectrolyte multilayers will be presented. For this purpose, three samples were prepared: The first film included Au ions as the outermost layer. For the other two films, ion-exchange was further followed by depositing one and two polyelectrolyte layer adsorption, respectively. When these three samples were subjected to 254 nm deep-UV irradiation for 12 hours, the optical changes which took places are given in Figure 28(II). For the film having Au ions as the outermost layer, the UV irradiation resulted in subsequent reduction of Au^{3+} and production of nanoparticles where the characteristic absorption band of Au is observed at 530 nm (Figure 28(II(a))). This film can also be patterned during the UV light exposure as it is shown in Figure

28(I). The contrast between the regions with and without gold nanoparticles can be seen clearly in the SEM image.

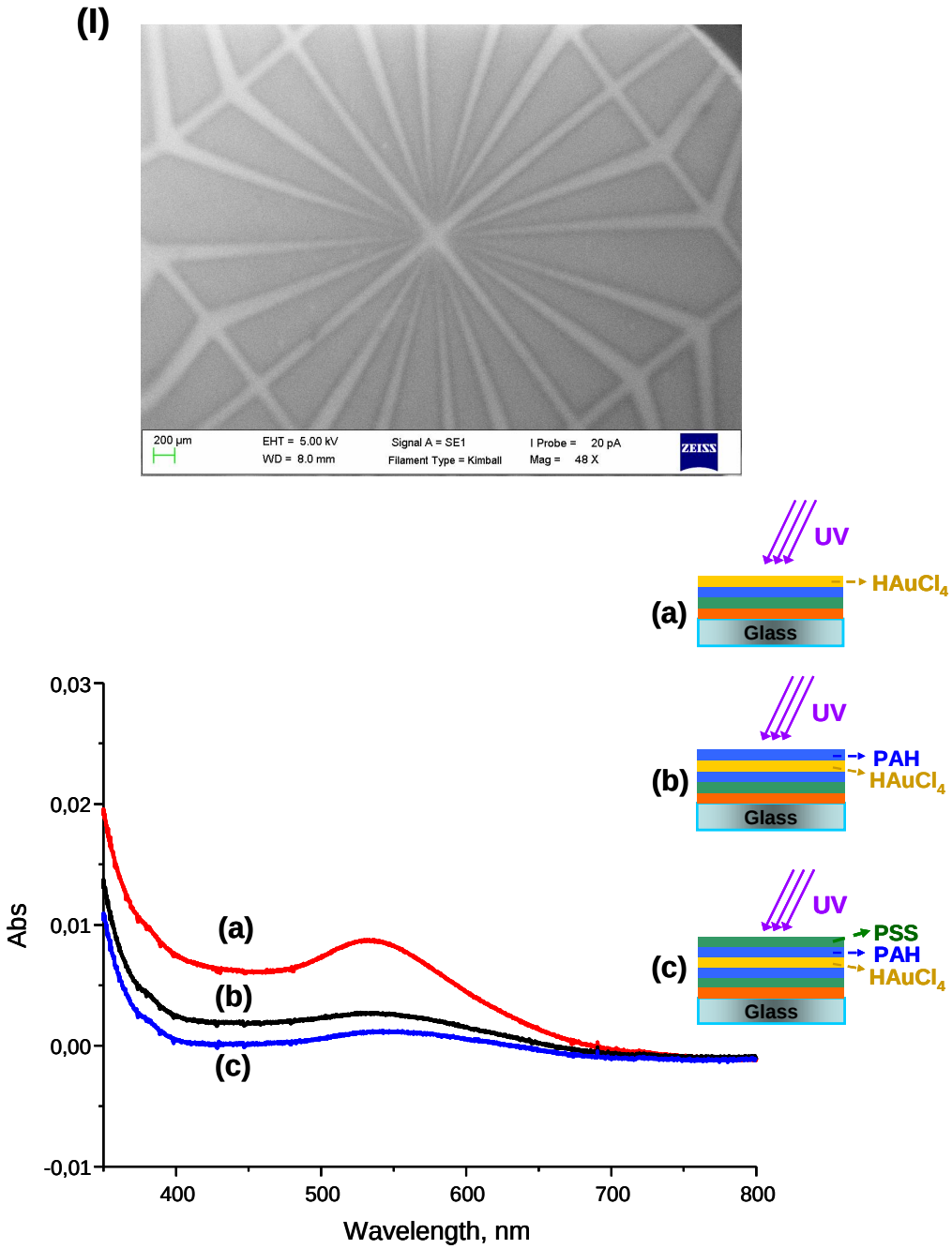

Figure 28. (I) SEM image of a patterened (PEI/PSS/PAH/$HAuCl_4$) film irradiated with UV light **(II)** UV-vis spectra of **(a)** (PEI/PSS/PAH/$HAuCl_4$) **(b)** (PEI/PSS/PAH/$HAuCl_4$/PAH) **(c)** (PEI/PSS/PAH/$HAuCl_4$/PAH/PSS) films irradiated with UV light.

When additional polyelectrolyte layers were deposited onto the outermost gold layer, absorption intensity decreased following the increase in the number of polyelectrolyte layers. We attribute this hindrance of nanocluster formation to be the result of restricted movement of metal ions in between charged polyelectrolyte layers. As it was shown by our group in a recent study, irradiation by X-ray and 254 nm deep-UV of gold salt in a PMMA film leads to reduction of gold ions and nanocluster formation takes place in a much longer time period which is evidenced by both XPS and UV-vis-NIR absorption spectroscopy.[94] Although the gold ions were distributed in between PMMA matrix, the cluster formation is established, but very slowly. Conversely, when gold ions were embedded in between polyelectrolyte layers, we believe that the charged polyelectrolytes limit the degree of aggregation, since we could not observe significant UV - absorption band around 520 nm. We must also state that particles having diameters smaller than 5 nm do not exhibit appreciable plasmon absorption; hence although the Au ions are reduced they may be present in small nanoclusters.

After gold ions were incorporated into polyelectrolyte matrix and irradiated with UV light, in order to see the effect of the temperature on particle aggregation, the samples were heated. It has been already established in the literature that increase of the temperature leads to increase in the growth rates of the nanoparticles in the polymeric matrix.[94] Accordingly, two samples were prepared. The first one contained gold ions as the outermost layer and the other one had two additional polyelectrolyte layers on top of gold. Both of the samples were irradiated with UV light for 12 hours and heated at 50ºC for again 12 hours as shown in Figure 29. In both samples, the absorbance of the SPR band of gold increased by applying heat, only marginally. It was reported in the PMMA matrix, absorbance of the SPR band of gold increases

drastically by applying heat.[94] The small amount of increase in the intensity of the SPR band may be attributed with again the 'charged' nature of our polymeric medium. The compact structure of the charged polyelectrolyte films might be one factor restricting the particle growth upon heating.

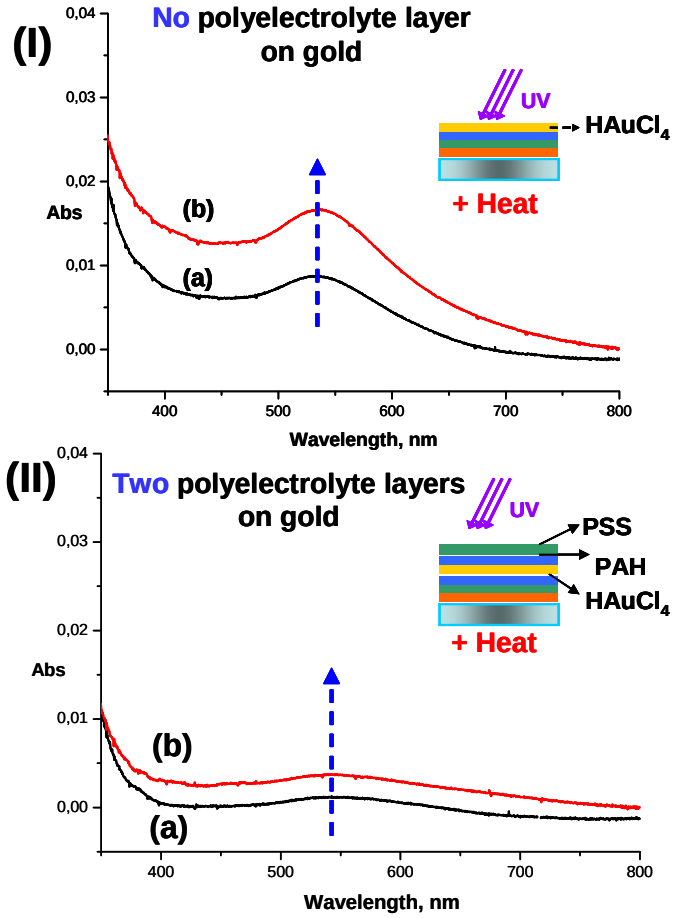

Figure 29. UV-Vis absorption spectra of **(I)** PEI/PSS/PAH/$HAuCl_4$ film irradiated with UV light **(a)** at room temperature **(b)** 50ºC and **(II)** PEI/PSS/PAH/$HAuCl_4$/PAH/PSS film irradiated with UV light **(a)** at room temperature **(b)** 50ºC.

3.3.3 X-ray Induced Reduction of Au Ions in Polyelectrolyte Matrices

Besides chemical treatments, H_2 exposure and UV-light irradiation, X-ray irradiation can also induce reduction of some metal ions. Although it is known that X-ray exposure causes various damages to the sample under investigation, the damage can also be utilized for reducing the metal ions, and in some cases creating nanoclusters.[95] The convenience of the XPS technique is that by using the X-ray beam for reduction, one can also follow the reduction of Au^{3+} to Au^0 while recording the data, which is facilitated by their large XPS chemical shifts.[94,95]

Accordingly, we have recorded XPS data during X-ray exposure of the gold ions incorporated into the polyelectrolyte multilayers. For this purpose, three separate samples were prepared. The first polyelectrolyte film included gold ions as the outermost layer. The second film had two additional polyelectrolyte layers on top of this Au^{3+} layer, and the last sample had the same ingredients, but was treated with UV irradiation for 12 h before XPS analysis.

Figure 30 shows the XPS spectra of the Au4f photoelectron region for these three samples, while the samples were subjected to X-rays. For the film having gold as the outermost layer, PEI/PSS/$HAuCl_4$, one can see that at the very beginning the Au4f region has a complex shape. This complex structure of the Au4f peak originates from the presence of the two different gold states, Au^{3+} and Au^0 (Figure 30(a)). At this early stage of the experiment (approximately after 2 minutes X-ray exposure), around 50% of the gold species has already been reduced. Continuing X-ray irradiation leads to a decrease in the intensity of Au^{3+} doublet and increase in the intensity of Au^0 one.

The second sample, PEI/PSS/PAH/$HAuCl_4$/PAH/PSS, was irradiated with X-rays and Figure 30(b) was obtained. At the early stages of the experiment, the shape

of the Au4f photoelectron peak is again complex but no significant variation can be observed compared to the first sample. A likely explanation could be that during the deposition of the additional polyelectrolyte layers partial reduction in the Au^{3+} due to amine groups in the PAH layer could have taken place. The complete reduction was established in few minutes after subjecting the sample to the X-rays. The last studied sample has the same order of species with a further UV treatment for 12 hours. XPS spectra showed that (Figure 30(c)) gold appeared only in the Au^0 state even at the very beginning of X-ray exposure. It is obvious that UV irradiation induced gold reduction, which is also confirmed by the UV-vis results. The reduction process can also be correlated with the decrease in the Cl2p peak intensity (Figure 31).

The Figure 31 depicts the survey spectra of the same three samples which were recorded after completing the X-ray (if any) reduction process. It was observed that the intensity ratio of the gold peaks in sample 1 and 2 is 4.7 ($I_1/I_2 = 4.7$). By using Equation (2), the thickness of the polyelectrolyte over layers can now be determined as 5 nm. This number is large compared to the 0.6 nm/layer that we have found in Section 3.1.3 for a single polyelectrolyte on Si/SiO_2. Under same conditions for a homogenous bilayered film, the expected thickness should be about 1.2 nm. But Lvov and co-workers reported that increase in salt concentration resulted with a drastic change in the thickness of the polyelectrolyte layers and not followed a linear behavior with respect to the NaCl concentration.[5] It is worth to mention that the solutions were prepared in higher NaCl concentration in the ion-exchange process compared to the deposition of polyelectrolyte layers on Si/SiO_2 and glass substrates. Caruso et al. demonstrated a similar irregular growth of polyelectrolyte layers below 4 layers.[73] Hence, our finding that the bilayer thickness of 5nm on top of the gold layer is not drastically different.

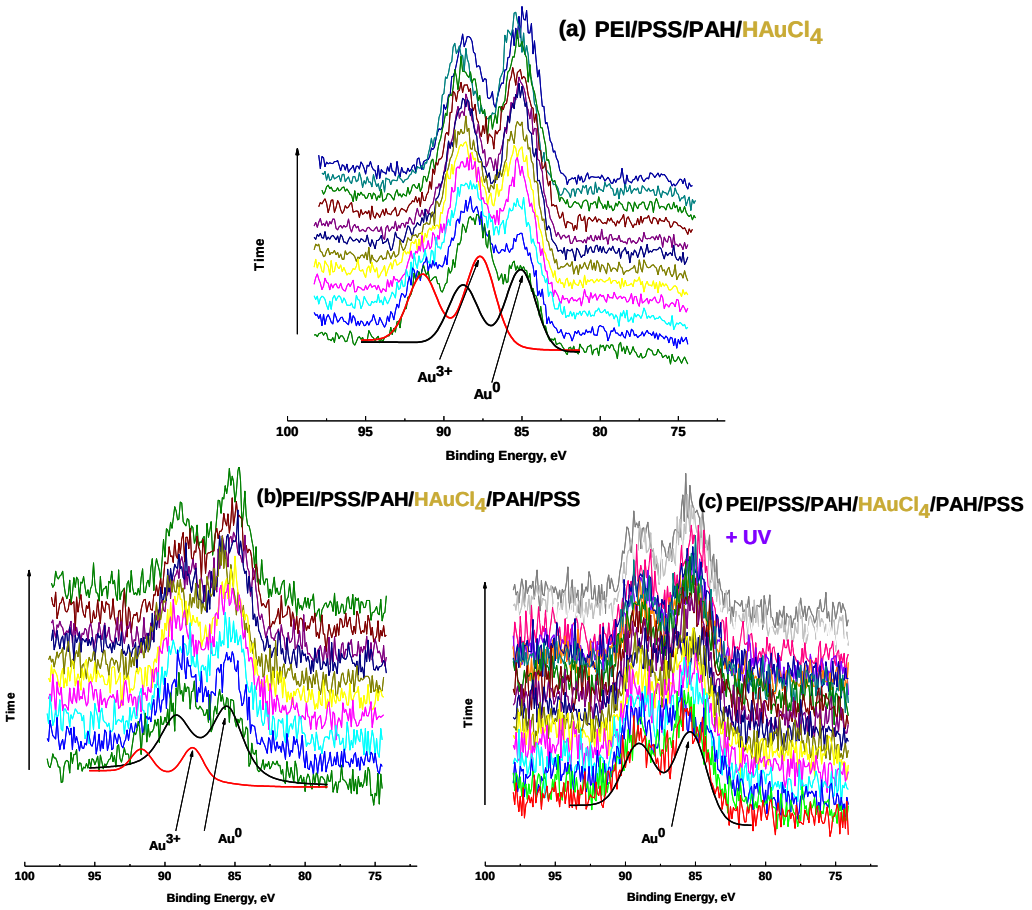

Figure 30. XPS spectra of Au4f region corresponding to **(a)** PEI/PSS/PAH/$HAuCl_4$ **(b)** PEI/PSS/PAH/$HAuCl_4$/PAH and **(c)** PEI/PSS/PAH/$HAuCl_4$/PAH/PSS films.

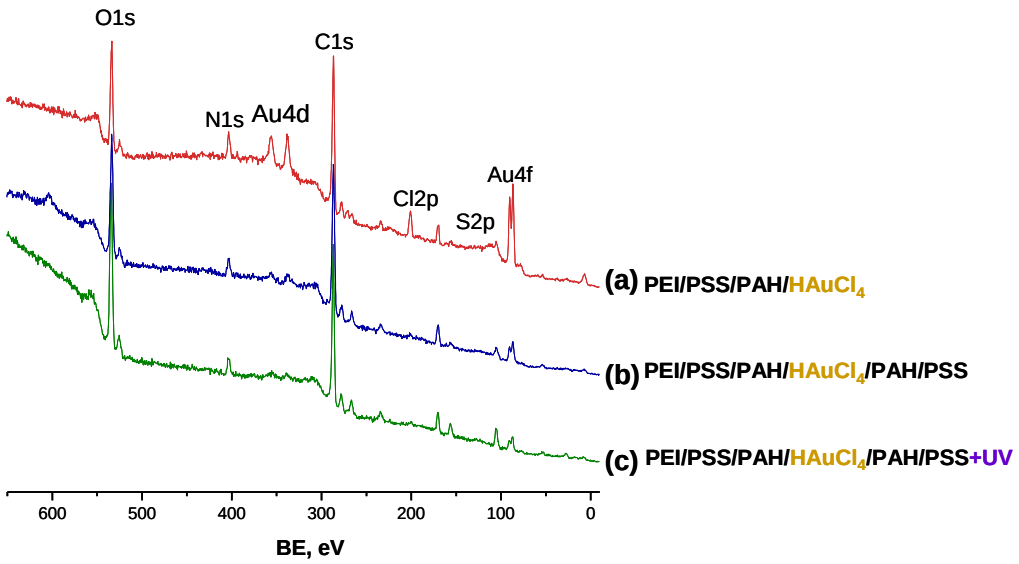

Figure 31. XPS survey spectra of **(a)** PEI/PSS/PAH/$HAuCl_4$, **(b)** PEI/PSS/PAH/$HAuCl_4$/PAH/PSS and **(c)** UV light irradiated PEI/PSS/PAH/$HAuCl_4$/PAH/PSS films.

As the main conclusion of this section, the experimental findings have shown that, once gold ions are incorporated into polyelectrolyte matrices, the reduction can be induced by utilizing UV and/or X-rays. The reduction, and in certain cases nanoparticle formation can be evidenced in-situ while recording XPS data. The shape and the chemical states of the corresponding peaks can give detailed information about the degree of reduction. The major purpose was to achieve structures containing gold ions which were incorporated via ion-exchange. We showed that without any chemical modification of the substrate or the polyelectrolyte, gold ions can be exchanged with Cl^- ions which serve as the counterions of PAH. It was demonstrated with a further UV light treatment, gold ions that are embedded in the polyelectrolyte matrix can also be converted to nanoparticles. However, if ion-exchange with metal salts was followed with additional polyelectrolyte deposition on top, it was shown that the aggregation of the reduced metallic ions became limited. This behavior was explained to be the result of restricted movement of metal ions in between charged polyelectrolyte layers. Similarly, reduction process was also followed by using X-ray beam, where a clear evolution of the chemical state of gold could be followed.

4. CONCLUSIONS

In this thesis, preparation and characterization of layer-by-layer assembled ultra-thin films were presented. The versatility of layer-by-layer approach gave us opportunity to prepare these ultra-thin films with different building blocks and investigate them using several spectroscopic techniques.

The study was focused on three major points: (i) characterization of layer-by-layer deposited ultra-thin polyelectrolyte layers on Si/SiO_2 substrate by XPS, (ii) incorporation of Au and/or Ag nanoparticles in between polyelectrolyte layers using LbL deposition and investigation of their optical responses by UV-vis absorption spectroscopy and, (iii) incorporation of Au ions into layer-by-layer assembled polyelectrolyte multilayers via ion-exchange and their subsequent reduction.

In the first part of this thesis, layer-by-layer deposited single and oppositely charged bilayered polyelectrolytes on Si/SiO_2 surface were investigated with XPS while applying an external bias. By switching the polarity of the applied potential, the underlying oxide layer was imposed to change from the positively and the negatively state. It was observed that a single charged polyelectrolyte layer, PAH, responded to that of electrical stimulus by rearranging their quaternary ammonium groups. When the oxide layer was negatively charged, the ammonium groups oriented towards to this oxide layer and in the case of the positively charged oxide layer, the positively charged groups on PAH moved towards to the outermost layer. This molecular reorientation was evidenced by the change in the intensity of the N1s signals. When an additional polyelectrolyte layer was deposited on top of the PAH layer, the change in the intensity of N1s signal was not observed due to the locking of the positively charged ammonium by negatively charged sulfonate groups corresponding to PSS layer.

Second part of the thesis presented optical responses of metal nanoparticle incorporated polyelectrolyte multilayers which were prepared through LbL assembly. It was shown that increase in the number of the gold layers leaded to a new contribution in the absorption spectrum at higher wavelengths besides the characteristic SPR band of gold. The same behavior was also observed for Ag incorporated films in multilayer assemblies. In order to understand the origin of this new band, three experimental approaches were followed; (i) increasing the number of the polyelectrolyte layers between gold layers, (ii) introducing another type of a metal nanoparticle in between polyelectrolyte layers in an alternate fashion and (iii) etching of the gold nanoparticles from multilayers selectively from the outermost layer. Following these strategies enabled us to conclude that involvement of a new band originated from the so-called 'interlayer interparticle interaction' which is the interaction of gold nanoparticles between adjacent layers. It was demonstrated that all of these experimental methods resulted in a decrease in the interparticle interaction and by using one of these methods; it is possible to control and manipulate the optical properties of these compact structures.

In the last part of the study, incorporation of gold ions into layer-by-layer deposited polyelectrolyte multilayers by use of ion-exchange method was reported. Once gold ions were introduced into polyelectrolyte layers, their subsequent reduction were achieved by irradiating the samples with either UV light or X-ray beam. In certain structural orders, the reduced ions were converted into nanoparticles which were evidenced by the characteristic SPR band of gold in the UV-absorption spectrum. When the reduction was followed with depositing additional polyelectrolyte layers on top of the gold layer, the nanoparticle formation was limited which was attributed to be the result of restricted movement of reduced ions in

between ‘charged’ polyelectrolyte layers. The reduction process was also followed in-situ while recording XPS data. The gold ions were reduced under X-ray beam and evidenced by the clear separate chemical states of Au^{3+} and Au^{0}. Continuing irradiation with the X-rays resulted with decrease in the intensity of the ionic gold signal and increase in the metallic state.

5. REFERENCES

1. Decher, G.; "Fuzzy Nanoassemblies: Toward Layered Polymeric Multicomposites" *Science* **1997,** 277(5330), 1232-1237.
2. Decher, G. S. J. B., "*Multilayer Thin Films: Sequential Assembly of Nanocomposite Materials"* Wiley-VCH: 2003; p 2-30.
3. Decher, G.; Hong, J. D.; Schmitt, J.; "Buildup of Ultrathin Multilayer Films by a Self-Assembly Process .3. Consecutively Alternating Adsorption of Anionic and Cationic Polyelectrolytes on Charged Surfaces" *Thin Solid Films* **1992,** 210(1-2), 831-835.
4. Schmitt, J.; Grunewald, T.; Decher, G.; Pershan, P. S.; Kjaer, K.; Losche, M.; "Internal Structure of Layer-by-Layer Adsorbed Polyelectrolyte Films - a Neutron and X-Ray Reflectivity Study" *Macromolecules* **1993,** 26(25), 7058-7063.
5. Lvov, Y.; Decher, G.; Sukhorukov, G.; "Assembly of Thin-Films by Means of Successive Deposition of Alternate Layers of DNA and Poly(Allylamine)" *Macromolecules* **1993,** 26(20), 5396-5399.
6. Liu, H.; Skibinska, L.; Gapinski, J.; Patkowski, A.; Fischer, E. W.; Pecora, R.; "Effect of Electrostatic Interactions on the Structure and Dynamics of a Model Polyelectrolyte. I. Diffusion" *Journal of Chemical Physics* **1998,** 109(17), 7556-7566.
7. Brender, C.; Danino, M.; "Screening in Short Polyelectrolyte Chains. A Monte Carlo Study" *Journal of Physical Chemistry* **1996,** 100(44), 17563-17567.
8. VonKlitzing, R.; Mohwald, H.; "A Realistic Diffusion Model for Ultrathin Polyelectrolyte Films" *Macromolecules* **1996,** 29(21), 6901-6906.
9. Lourenco, J. M. C.; Ribeiro, P. A.; do Rego, A. M. B.; Fernandes, F. M. B.; Moutinho, A. M. C.; Raposo, M.; "Counterions in Poly(Allylamine Hydrochloride) and Poly(Styrene Sulfonate) Layer-by-Layer Films" *Langmuir* **2004,** 20(19), 8103-8109.
10. http://pslc.ws/macrog/electro.htm.
11. Farhat, T.; Yassin, G.; Dubas, S. T.; Schlenoff, J. B.; "Water and Ion Pairing in Polyelectrolyte Multilayers" *Langmuir* **1999,** 15(20), 6621-6623.

12. Schlenoff, J. B.; Dubas, S. T.; "Mechanism of Polyelectrolyte Multilayer Growth: Charge Overcompensation and Distribution" *Macromolecules* **2001,** 34(3), 592-598.

13. Bertrand, P.; Jonas, A.; Laschewsky, A.; Legras, R.; "Ultrathin Polymer Coatings by Complexation of Polyelectrolytes at Interfaces: Suitable Materials, Structure and Properties" *Macromolecular Rapid Communications* **2000,** 21(7), 319-348.

14. Caruso, F.; Lichtenfeld, H.; Donath, E.; Mohwald, H.; "Investigation of Electrostatic Interactions in Polyelectrolyte Multilayer Films: Binding of Anionic Fluorescent Probes to Layers Assembled onto Colloids" *Macromolecules* **1999,** 32(7), 2317-2328.

15. Hoogeveen, N. G.; Stuart, M. A. C.; Fleer, G. J.; Bohmer, M. R.; "Formation and Stability of Multilayers of Polyelectrolytes" *Langmuir* **1996,** 12(15), 3675-3681.

16. Ramsden, J. J.; Lvov, Y. M.; Decher, G.; "Determination of Optical-Constants of Molecular Films Assembled Via Alternate Polyion Adsorption" *Thin Solid Films* **1995,** 254(1-2), 246-251.

17. Freeman, R. G.; Grabar, K. C.; Allison, K. J.; Bright, R. M.; Davis, J. A.; Guthrie, A. P.; Hommer, M. B.; Jackson, M. A.; Smith, P. C.; Walter, D. G.; Natan, M. J.; "Self-Assembled Metal Colloid Monolayers - an Approach to SERS Substrates" *Science* **1995,** 267(5204), 1629-1632.

18. Schmitt, J.; Decher, G.; Dressick, W. J.; Brandow, S. L.; Geer, R. E.; Shashidhar, R.; Calvert, J. M.; "Metal Nanoparticle/Polymer Superlattice Films: Fabrication and Control of Layer Structure" *Advanced Materials* **1997,** 9(1), 61-&.

19. Schlenoff, J. B.; Dubas, S. T.; Farhat, T.; "Sprayed Polyelectrolyte Multilayers" *Langmuir* **2000,** 16(26), 9968-9969.

20. Cho, J.; Char, K.; Hong, J. D.; Lee, K. B.; "Fabrication of Highly Ordered Multilayer Films Using a Spin Self-Assembly Method" *Advanced Materials* **2001,** 13(14), 1076-1078.

21. Lee, S. S.; Hong, J. D.; Kim, C. H.; Kim, K.; Koo, J. P.; Lee, K. B.; "Layer-by-Layer Deposited Multilayer Assemblies of Ionene-Type Polyelectrolytes Based on the Spin-Coating Method" *Macromolecules* **2001,** 34(16), 5358-5360.

22. Chiarelli, P. A.; Johal, M. S.; Casson, J. L.; Roberts, J. B.; Robinson, J. M.; Wang, H. L.; "Controlled Fabrication of Polyelectrolyte Multilayer Thin Films Using Spin-Assembly" *Advanced Materials* **2001,** 13(15), 1167-1171.

23. Hammond, P. T.; "Form and Function in Multilayer Assembly: New Applications at the Nanoscale" *Advanced Materials* **2004,** 16(15), 1271-1293.

24. Quinn, J. F.; Johnston, A. P. R.; Such, G. K.; Zelikin, A. N.; Caruso, F.; "Next Generation, Sequentially Assembled Ultrathin Films: Beyond Electrostatics" *Chemical Society Reviews* **2007,** 36(5), 707-718.

25. Azzaroni, O.; Brown, A. A.; Huck, W. T. S.; "Tunable Wettability by Clicking into Polyelectrolyte Brushes" *Advanced Materials* **2007,** 19(1), 151-154.

26. Lee, B. S.; Chi, Y. S.; Lee, J. K.; Choi, I. S.; Song, C. E.; Namgoong, S. K.; Lee, S. G.; "Imidazolium Ion-Terminated Self-Assembled Monolayers on Au: Effects of Counteranions on Surface Wettability" *Journal of the American Chemical Society* **2004,** 126(2), 480-481.

27. Shen, Y. F.; Zhang, Y. J.; Zhang, Q. X.; Niu, L.; You, T. Y.; Ivaska, A.; "Immobilization of Ionic Liquid with Polyelectrolyte as Carrier" *Chemical Communications* **2005,** (33), 4193-4195.

28. Liming Wang, Y. L., Bo Peng and Zhaohui Su; "Tunable Wettability by Counterion Exchange at the Surface of Electrostatic Self-Assembled Multilayers" *Chemical Communications* **2008,** 5972 - 5974.

29. Chia, K. K.; Cohen, R. E.; Rubner, M. F.; "Amine-Rich Polyelectrolyte Multilayer Nanoreactors for In Situ Gold Nanoparticle Synthesis" *Chemistry of Materials* **2008,** 20(21), 6756-6763.

30. Ozkaraoglu, E.; Tunc, I.; Suzer, S.; "X-Ray Induced Reduction of Au and Pt Ions on Silicon Substrates" *Surface & Coatings Technology* **2007,** 201(19-20), 8202-8204.

31. Burda, C.; Chen, X. B.; Narayanan, R.; El-Sayed, M. A.; "Chemistry and Properties of Nanocrystals of Different Shapes" *Chemical Reviews* **2005,** 105(4), 1025-1102.

32. Kozlovskaya, V.; Kharlampieva, E.; Khanal, B. P.; Manna, P.; Zubarev, E. R.; Tsukruk, V. V.; "Ultrathin Layer-by-Layer Hydrogels with Incorporated Gold Nanorods as pH-Sensitive Optical Materials" *Chemistry of Materials* **2008,** 20(24), 7474-7485.

33. Lee, D.; Rubner, M. F.; Cohen, R. E.; "All-Nanoparticle Thin-Film Coatings" *Nano Letters* **2006,** 6(10), 2305-2312.

34. Ostrander, J. W.; Mamedov, A. A.; Kotov, N. A.; "Two Modes of Linear Layer-by-Layer Growth of Nanoparticle-Polylectrolyte Multilayers and Different Interactions in the Layer-by-Layer Deposition" *Journal of the American Chemical Society* **2001,** 123(6), 1101-1110.

35. Lvov, Y.; Ariga, K.; Onda, M.; Ichinose, I.; Kunitake, T.; "Alternate Assembly of Ordered Multilayers of SiO_2 and Other Nanoparticles and Polyions" *Langmuir* **1997,** 13(23), 6195-6203.

36. Caruso, R. A.; Susha, A.; Caruso, F.; "Multilayered Titania, Silica, and Laponite Nanoparticle Coatings on Polystyrene Colloidal Templates and Resulting Inorganic Hollow Spheres" *Chemistry of Materials* **2001,** 13(2), 400-409.

37. Krasteva, N.; Besnard, I.; Guse, B.; Bauer, R. E.; Mullen, K.; Yasuda, A.; Vossmeyer, T.; "Self-Assembled Gold Nanoparticle/Dendrimer Composite Films for Vapor Sensing Applications" *Nano Letters* **2002,** 2(5), 551-555.

38. Park, J.; Fouche, L. D.; Hammond, P. T.; "Multicomponent Patterning of Layer-by-Layer Assembled Polyelectrolyte/Nanoparticle Composite Thin Films with Controlled Alignment" *Advanced Materials* **2005,** 17(21), 2575-2579.

39. Henglein, A.; "Radiolytic Preparation of Ultrafine Colloidal Gold Particles in Aqueous Solution: Optical Spectrum, Controlled Growth, and Some Chemical Reactions" *Langmuir* **1999,** 15(20), 6738-6744.

40. Henglein, A.; Meisel, D.; "Radiolytic Control of the Size of Colloidal Gold Nanoparticles" *Langmuir* **1998,** 14(26), 7392-7396.

41. Link, S.; El-Sayed, M. A.; "Size and Temperature Dependence of the Plasmon Absorption of Colloidal Gold Nanoparticles" *Journal of Physical Chemistry B* **1999,** 103(21), 4212-4217.

42. Mulvaney, P.; "Surface Plasmon Spectroscopy of Nanosized Metal Particles" *Langmuir* **1996,** 12(3), 788-800.

43. Kamat, P. V.; "Photophysical, Photochemical and Photocatalytic Aspects of Metal Nanoparticles" *Journal of Physical Chemistry B* **2002,** 106(32), 7729-7744.

44. Link, S.; El-Sayed, M. A.; "Spectral Properties and Relaxation Dynamics of Surface Plasmon Electronic Oscillations in Gold and Silver Nanodots and Nanorods" *Journal of Physical Chemistry B* **1999,** 103(40), 8410-8426.

45. Liz-Marzan, L. M.; "Tailoring Surface Plasmons through the Morphology and Assembly of Metal Nanoparticles" *Langmuir* **2006,** 22(1), 32-41.

46. Mallin, M. P.; Murphy, C. J.; "Solution-Phase Synthesis of Sub-10 nm Au-Ag Alloy Nanoparticles" *Nano Letters* **2002,** 2(11), 1235-1237.

47. Rodriguez-Gonzalez, B.; Sanchez-Iglesias, A.; Giersig, M.; Liz-Marzan, L. M. In *Auag Bimetallic Nanoparticles: Formation, Silica-Coating and Selective Etching*, 2004; 2004; pp 133-144.

48. Mulvaney, P.; Giersig, M.; Henglein, A.; "Electrochemistry of Multilayer Colloids - Preparation and Absorption-Spectrum of Gold-Coated Silver Particles" *Journal of Physical Chemistry* **1993,** 97(27), 7061-7064.

49. Lu, L. H.; Wang, H. S.; Zhou, Y. H.; Xi, S. Q.; Zhang, H. J.; Jiawen, H. B. W.; Zhao, B.; "Seed-Mediated Growth of Large, Monodisperse Core-Shell Gold-Silver Nanoparticles with Ag-Like Optical Properties" *Chemical Communications* **2002,** (2), 144-145.

50. Rodriguez-Gonzalez, B.; Burrows, A.; Watanabe, M.; Kiely, C. J.; Liz-Marzan, L. M.; "Multishell Bimetallic Auag Nanoparticles: Synthesis, Structure and Optical Properties" *Journal of Materials Chemistry* **2005,** 15(17), 1755-1759.

51. Underwood, S.; Mulvaney, P.; "Effect of the Solution Refractive-Index on the Color of Gold Colloids" *Langmuir* **1994,** 10(10), 3427-3430.

52. Jiang, C. Y.; Markutsya, S.; Tsukruk, V. V.; "Collective and Individual Plasmon Resonances in Nanoparticle Films Obtained by Spin-Assisted Layer-by-Layer Assembly" *Langmuir* **2004,** 20(3), 882-890.

53. Felidj, N.; Aubard, J.; Levi, G.; Krenn, J. R.; Salerno, M.; Schider, G.; Lamprecht, B.; Leitner, A.; Aussenegg, F. R.; "Controlling the Optical Response of Regular Arrays of Gold Particles for Surface-Enhanced Raman Scattering" *Physical Review B* **2002,** 65(7), 075419(9).

54. Taleb, A.; Petit, C.; Pileni, M. P.; "Optical Properties of Self-Assembled 2d and 3d Superlattices of Silver Nanoparticles" *Journal of Physical Chemistry B* **1998,** 102(12), 2214-2220.

55. Fu, Y.; Xu, H.; Bai, S. L.; Qiu, D. L.; Sun, J. Q.; Wang, Z. Q.; Zhang, X.; "Fabrication of a Stable Polyelectrolyte/Au Nanoparticles Multilayer Film" *Macromolecular Rapid Communications* **2002,** 23(4), 256-259.

56. Ung, T.; Liz-Marzan, L. M.; Mulvaney, P.; "Optical Properties of Thin Films of Au@SiO_2 Particles" *Journal of Physical Chemistry B* **2001,** 105(17), 3441-3452.

57. Pastoriza-Santos, I.; Scholer, B.; Caruso, F.; "Core-Shell Colloids and Hollow Polyelectrolyte Capsules Based on Diazoresins" *Advanced Functional Materials* **2001,** 11(2), 122-128.

58. Malikova, N.; Pastoriza-Santos, I.; Schierhorn, M.; Kotov, N. A.; Liz-Marzan, L. M.; "Layer-by-Layer Assembled Mixed Spherical and Planar Gold Nanoparticles: Control of Interparticle Interactions" *Langmuir* **2002,** 18(9), 3694-3697.

59. Mayya, K. S.; Schoeler, B.; Caruso, F.; "Preparation and Organization of Nanoscale Polyelectrolyte-Coated Gold Nanoparticles" *Advanced Functional Materials* **2003,** 13(3), 183-188.

60. Gittins, D. I.; Caruso, F.; "Tailoring the Polyelectrolyte Coating of Metal Nanoparticles" *Journal of Physical Chemistry B* **2001,** 105(29), 6846-6852.

61. Briggs, D. S., M. P.,, "*Practical Surface Analysis. Part I. Auger and X-Ray Photoelectron Spectroscopy"* 2nd Edition ed.; John Wiley & Sons Ltd.: London, 1996.

62. Bonzel, H. P.; Kleint, C.; "On the History of Photoemission" *Progress in Surface Science* **1995,** 48(1-4), 179-179.

63. Iwata, S.; Ishizaka, A.; "Electron Spectroscopic Analysis of the SiO_2/Si System and Correlation with Metal-Oxide-Semiconductor Device Characteristics" *Journal of Applied Physics* **1996,** 79(9), 6653-6713.

64. Ulgut, B.; Suzer, S.; "XPS Studies of SiO_2/Si System under External Bias" *Journal of Physical Chemistry B* **2003,** 107(13), 2939-2943.

65. Lau, W. M.; Wu, X. W.; "Measurements of Interface State Density by X-Ray Photoelectron-Spectroscopy" *Surface Science* **1991,** 245(3), 345-352.

66. Suzer, S.; "Differential Charging in X-Ray Photoelectron Spectroscopy: A Nuisance or a Useful Tool?" *Analytical Chemistry* **2003,** 75(24), 7026-7029.

67. Karadas, F.; Ertas, G.; Suzer, S.; "Differential Charging in SiO_2/Si System as Determined by XPS" *Journal of Physical Chemistry B* **2004,** 108(4), 1515-1518.

68. Dubey, M.; Gouzman, I.; Bernasek, S. L.; Schwartz, J.; "Characterization of Self-Assembled Organic Films Using Differential Charging in X-Ray Photoelectron Spectroscopy" *Langmuir* **2006,** 22(10), 4649-4653.

69. Conger, C. P.; Suzer, S.; "Response of Polyelectrolyte Layers to the SiO_2 Substrate Charging as Probed by XPS" *Langmuir* **2009,** 25(3), 1757-1760.

70. Tagliazucchi, M.; Williams, F. J.; Calvo, E. J.; "Effect of Acid-Base Equilibria on the Donnan Potential of Layer-by-Layer Redox Polyelectrolyte Multilayers" *Journal of Physical Chemistry B* **2007,** 111(28), 8105-8113.

71. Liu, J. W.; Li, X. J.; Schrand, A.; Ohashi, T.; Dai, L. M.; "Controlled Syntheses of Aligned Multi-Walled Carbon Nanotubes: Catalyst Particle Size and Density Control Via Layer-by-Layer Assembling" *Chemistry of Materials* **2005,** 17(26), 6599-6604.

72. Kidambi, S.; Bruening, M. L.; "Multilayered Polyelectrolyte Films Containing Palladium Nanoparticles: Synthesis, Characterization, and Application in Selective Hydrogenation" *Chemistry of Materials* **2005,** 17(2), 301-307.

73. Caruso, F.; Niikura, K.; Furlong, D. N.; Okahata, Y.; "Ultrathin Multilayer Polyelectrolyte Films on Gold: Construction and Thickness Determination .1" *Langmuir* **1997,** 13(13), 3422-3426.

74. Hsieh, M. C.; Farris, R. J.; McCarthy, T. J.; "Surface "Priming" For Layer-by-Layer Deposition: Polyelectrolyte Multilayer Formation on Allylamine Plasma-Modified Poly(Tetrafluoroethylene)" *Macromolecules* **1997,** 30(26), 8453-8458.

75. Ghosal, S.; Hemminger, J. C.; Bluhm, H.; Mun, B. S.; Hebenstreit, E. L. D.; Ketteler, G.; Ogletree, D. F.; Requejo, F. G.; Salmeron, M.; "Electron Spectroscopy of Aqueous Solution Interfaces Reveals Surface Enhancement of Halides" *Science* **2005,** 307(5709), 563-566.

76. Maier, F.; Gottfried, J. M.; Rossa, J.; Gerhard, D.; Schulz, P. S.; Schwieger, W.; Wasserscheid, P.; Steinruck, H. P.; "Surface Enrichment and Depletion Effects of Ions Dissolved in an Ionic Liquid: An X-Ray Photoelectron Spectroscopy Study" *Angewandte Chemie-International Edition* **2006,** 45(46), 7778-7780.

77. Doron-Mor, H.; Hatzor, A.; Vaskevich, A.; van der Boom-Moav, T.; Shanzer, A.; Rubinstein, I.; Cohen, H.; "Controlled Surface Charging as a Depth-Profiling Probe for Mesoscopic Layers" *Nature* **2000,** 406(6794), 382-385.

78. Shabtai, K.; Rubinstein, I.; Cohen, S. R.; Cohen, H.; "High-Resolution Lateral Differentiation Using a Macroscopic Probe: XPS of Organic Monolayers on Composite Au-SiO_2 Surfaces" *Journal of the American Chemical Society* **2000,** 122(20), 4959-4962.

79. Cohen, H.; "Chemically Resolved Electrical Measurements Using X-Ray Photoelectron Spectroscopy" *Applied Physics Letters* **2004,** 85(7), 1271-1273.

80. Gouzman, I.; Dubey, M.; Carolus, M. D.; Schwartz, J.; Bernasek, S. L.; "Monolayer Vs. Multilayer Self-Assembled Alkylphosphonate Films: X-Ray Photoelectron Spectroscopy Studies" *Surface Science* **2006,** 600(4), 773-781.

81. Ertas, G.; Suzer, S.; "XPS Analysis with External Bias: A Simple Method for Probing Differential Charging" *Surface and Interface Analysis* **2004,** 36(7), 619-623.

82. Demirok, U. K.; Ertas, G.; Suzer, S.; "Time-Resolved XPS Analysis of the SiO_2/Si System in the Millisecond Range" *Journal of Physical Chemistry B* **2004,** 108(17), 5179-5181.

83. Ertas, G.; Demirok, U. K.; Atalar, A.; Suzer, S.; "X-Ray Photoelectron Spectroscopy for Resistance-Capacitance Measurements of Surface Structures" *Applied Physics Letters* **2005,** 86(18), 183110.

84. Goh, S. H.; Lee, S. Y.; Zhou, X.; Tan, K. L.; "X-Ray Photoelectron Spectroscopic Studies of Interactions between Poly(4-Vinylpyridine) and Poly(Styrenesulfonate) Salts" *Macromolecules* **1998,** 31(13), 4260-4264.

85. Islam, A.; Mukherjee, M.; "Characterization of Langmuir-Blodgett Film Using Differential Charging in X-Ray Photoelectron Spectroscopy" *Journal of Physical Chemistry B* **2008,** 112(29), 8523-8529.

86. Cohen, H.; Maoz, R.; Sagiv, J.; "Transient Charge Accumulation in a Capacitive Self-Assembled Monolayer" *Nano Letters* **2006,** 6(11), 2462-2466.

87. Lahann, J.; Mitragotri S.; Tran T. N.; Kaido H.; Sundaram J.; Choi I. S.; Hoffer S.; Somorjai G. A.; Langer R.; "A Reversibly Switching Surface" *Science* **2003,** 299(5605), 371-374.

88. Bain, C. D.; Whitesides, G. M.; "Attenuation Lengths of Photoelectrons in Hydrocarbon Films" *Journal of Physical Chemistry* **1989,** 93(4), 1670-1673.

89. Schneider, G.; Decher, G.; Nerambourg, N.; Praho, R.; Werts, M. H. V.; Blanchard-Desce, M.; "Distance-Dependent Fluorescence Quenching on Gold Nanoparticles Ensheathed with Layer-by-Layer Assembled Polyelectrolytes" *Nano Letters* **2006,** 6(3), 530-536.

90. Dai, J. H.; Bruening, M. L.; "Catalytic Nanoparticles Formed by Reduction of Metal Ions in Multilayered Polyelectrolyte Films" *Nano Letters* **2002,** 2(5), 497-501.

91. Joseph B. Schlenoff, H. L., Ming Li; "Charge and Mass Balance in Polyelectrolyte Multilayers" *Journal of American Chemical Society* **1998,** 120 7626-7634.

92. Wang, T. C.; Rubner, M. F.; Cohen, R. E.; "Polyelectrolyte Multilayer Nanoreactors for Preparing Silver Nanoparticle Composites: Controlling Metal Concentration and Nanoparticle Size" *Langmuir* **2002,** 18(8), 3370-3375.

93. Esumi, K.; Suzuki, A.; Aihara, N.; Usui, K.; Torigoe, K.; "Preparation of Gold Colloids with UV Irradiation Using Dendrimers as Stabilizer" *Langmuir* **1998,** 14(12), 3157-3159.

94. Ozkaraoglu, E.; Tunc, K.; Suzer, S.; "Preparation of Au and Au-Pt Nanoparticles within Pmma Matrix Using UV and X-Ray Irradiation" *Polymer* **2009,** 50(2), 462-466.

95. Karadas, F.; Ertas, G.; Ozkaraoglu, E.; Suzer, S.; "X-Ray-Induced Production of Gold Nanoparticles on a SiO_2/Si System and in a Poly(Methyl Methacrylate) Matrix" *Langmuir* **2005,** 21(1), 437-442.

96. Logar, M.; Jancar, B.; Suvorov, D.; Kostanjsek, R.; "In Situ Synthesis of Ag Nanoparticles in Polyelectrolyte Multilayers" *Nanotechnology* **2007,** 18(32).